JGR Solid Earth

RESEARCH ARTICLE
10.1029/2021JB022170

High-Resolution Ps Receiver Function Imaging of the Crust and Mantle Lithosphere Beneath Southern New England and Tectonic Implications

Yantao Luo[1], Maureen D. Long[1], Paul Karabinos[2], Yvette D. Kuiper[3], Stéphane Rondenay[4], John C. Aragon[1,5], Lucas Sawade[4,6], and Peter Makus[4,7]

[1]Department of Earth and Planetary Sciences, Yale University, New Haven, CT, USA, [2]Department of Geosciences, Williams College, Williamstown, MA, USA, [3]Department of Geology and Geological Engineering, Colorado School of Mines, Golden, CO, USA, [4]Department of Earth Science, University of Bergen, Bergen, Norway, [5]Now at Earthquake Science Center, U.S. Geological Survey, Menlo Park, CA, USA, [6]Now at Department of Geosciences, Princeton University, Princeton, NJ, USA, [7]Now at GFZ German Research Center for Geosciences, Potsdam, Germany

Key Points:

- We conducted Ps receiver function analysis on a dense seismic array across northern Connecticut to investigate lithospheric structures
- We observe a step-like change in Moho depth near the boundary between Laurentia and the Gondwana-derived Moretown terrane
- Several seismic discontinuities within the lithosphere have implications for the complicated tectonic history of southern New England

Correspondence to:
Y. Luo,
yantao.luo@yale.edu

Citation:
Luo, Y., Long, M. D., Karabinos, P., Kuiper, Y. D., Rondenay, S., Aragon, J. C., et al. (2021). High-resolution Ps receiver function imaging of the crust and mantle lithosphere beneath southern New England and tectonic implications. *Journal of Geophysical Research: Solid Earth*, *126*, e2021JB022170. https://doi.org/10.1029/2021JB022170

Received 2 APR 2021
Accepted 3 JUL 2021

Abstract Southern New England exhibits diverse geologic features resulting from past tectonic events. These include Proterozoic and early Paleozoic Laurentian units in the west, several Gondwana-derived terranes that accreted during the Paleozoic in the east, and the Mesozoic Hartford Basin in the central part of the region. The Seismic Experiment for Imaging Structure beneath Connecticut (SEISConn) project involved the deployment of a dense array of 15 broadband seismometers across northern Connecticut to investigate the architecture of lithospheric structures beneath this region and interpret how they were created and modified by past tectonic events in the context of surface geology. We carried out P-to-S receiver function analysis on SEISConn data, including both single-station analysis and common conversion point (CCP) stacking. Our images show that the westernmost part of Connecticut has a much deeper Moho than central and eastern Connecticut. The lateral transition is a well-defined, ~15 km step-like offset of the Moho over a ~20 km horizontal distance. The Moho step appears near the surface boundary between the Laurentian margin and the Gondwana-derived Moretown terrane. Possible models for its formation include Ordovician underthrusting of Laurentia and/or modification by younger tectonic events. Other prominent features include a strong positive velocity gradient (PVG) beneath the Hartford basin corresponding to the bottom of the sedimentary units, several west-dipping PVGs in the crust and mantle lithosphere that may correspond to relict slabs or shear zones from past subduction episodes, and a negative velocity gradient (NVG) that may correspond to the base of the lithosphere.

Plain Language Summary The eastern margin of North America has a complicated tectonic history. It has been shaped by past episodes of landmasses coming together to form a supercontinent, with later breakup of the supercontinent to form a new ocean basin. This supercontinent cycle involves fundamental plate tectonic processes including subduction, the accretion of geologic microcontinents, the formation of mountain ranges, and rifting during the breakup of continents. These processes have led to the complex geology of southern New England that is visible at the surface, and they have also likely modified the deep structures of the crust and upper mantle. In this study, we analyzed data from seismometers deployed across northern Connecticut to investigate underground interfaces separating layers with different properties. We measured seismic waves from distant earthquakes and looked for evidence of specific wave behavior at these interfaces. We found that the interface separating the crust and the mantle, known as the Moho, is not continuous beneath this region. The Moho is much deeper in the west of our study area than in the east, and the transition from thick to thin crust corresponds to a key geologic boundary. We also identified several other interfaces, providing information on past tectonic events.

1. Introduction

Subduction, terrane accretion, and continental rifting are fundamental plate tectonic processes. Geologic features such as igneous rocks produced during arc magmatism, terrane boundaries separating regions with different origins, and rift basins filled with sedimentary units reflect such tectonic processes. It is likely

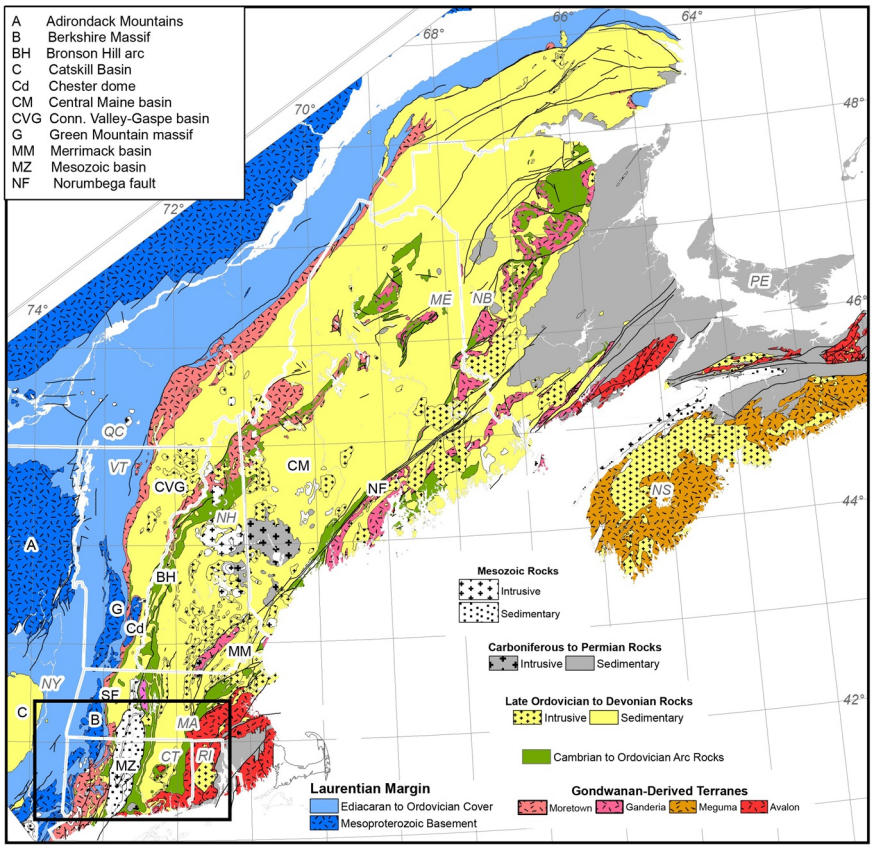

Figure 1. Tectonic map of the northern Appalachians, after Hibbard et al. (2006), and Karabinos et al. (2017). Black box at the bottom left corner denotes the boundaries of the station map shown in Figure 2. Locations of U.S. states and Canadian provinces are shown with abbreviations in italics (CT, Connecticut; MA, Massachusetts; RI, Rhode Island; VT, Vermont; NH, New Hampshire; ME, Maine; NY, New York; QC, Quebec; NB, New Brunswick; PE, Prince Edward Island; NS, Nova Scotia).

that these tectonic events also modify the structure of the crust and lithospheric mantle deep beneath the surface. Characterizing the structure of the crust and mantle lithosphere and correlating first-order features with surface geology can refine our understanding of key plate tectonic processes and help unravel the tectonic history of complex regions. In this study, we focus on southern New England, which was affected by Neoproterozoic rifting of Rodinia, terrane accretion during multiple phases of the Appalachian orogenic cycle, and by continental rifting during the breakup of Pangea. We applied receiver function analysis to data gathered from a high-density seismic array deployed across Connecticut, producing detailed images of the crust and mantle lithosphere that can be interpreted in light of constraints provided by studies of the geological units exposed at the surface.

1.1. Tectonic Setting of Southern New England

The eastern margin of North America has been shaped by two complete supercontinent cycles, the Mesoproterozoic Grenville orogenic cycle and the Paleozoic Appalachian orogenic cycle. The Grenville orogenic cycle led to the formation of the supercontinent Rodinia, followed by Neoproterozoic continental rifting; the Appalachian orogenic cycle led to the formation of the supercontinent Pangea, followed by Mesozoic rifting during the breakup of Pangea (Bogdanova et al., 2009; Hatcher, 2010; Rivers, 1997; Thomas, 2006; Withjack & Schlische, 2005). These past events are documented in the complex geologic record of southern New England (Figure 1).

The westmost portion of southern New England is on the margin of (pre-Appalachian) Laurentia, with exposed Mesoproterozoic crustal rocks of the Grenville orogenic belt (Karabinos & Aleinikoff, 1990; Karabinos

et al., 2008). The Grenville orogenic cycle was a series of Mesoproterozoic mountain-building events, which culminated in the formation of the supercontinent Rodinia. Following the Neoproterozoic breakup of Rodinia (Bogdanova et al., 2009; Rivers, 1997; Tollo et al., 2004), several orogenies led to the assembly of Gondwana (e.g., Meert & Van Der Voo, 1997). The collision of Laurentia with several Gondwana-derived terranes and subsequently with Gondwana composed the main episodes of the Paleozoic Appalachian orogenic cycle (Hatcher, 2010; Hibbard et al., 2010), which affected the entire eastern margin of North America.

The Moretown terrane, located just to the east of the Laurentian margin, is a Gondwana-derived terrane that was accreted to Laurentia during the Ordovician Taconic orogeny, the first episode of the Appalachian orogenic cycle (Macdonald et al., 2014). The Shelburne Falls magmatic arc, currently located west of the Hartford basin, was formed on the Moretown terrane as it approached Laurentia via an east-dipping subduction zone. The younger Bronson Hill magmatic arc, currently located east of the Hartford basin, may have also formed on the Moretown terrane, but probably above a west-dipping subduction zone (Karabinos et al., 2017). Karabinos et al. (2017) suggested that there was a reversal in subduction polarity during the Taconic orogeny from east- to west-dipping after the accretion of the Moretown terrane and the breakoff of the east-dipping lithospheric slab. To the east of the Bronson Hill magmatic arc, the surface is largely covered by Late Ordovician to Early Devonian rocks deformed during the latest Silurian to Middle Devonian Acadian orogeny (e.g., Hatcher, 2010; Karabinos et al., 2017; Nance et al., 2008; Skehan & Rast, 1990; van Staal et al., 2009). Another Gondwana-derived terrane, Ganderia, accreted during the Late Ordovician to Early Silurian Salinic orogeny (van Staal et al., 2009). Although Ganderia is well exposed in parts of the Canadian Appalachians (van Staal et al., 2009), it is largely covered by younger sedimentary rocks in southern New England (Figure 1). Nevertheless, recent geochemical evidence for a Ganderian affinity of the Nashoba terrane in southeastern New England suggests that Ganderia may extend farther to the southeast than previously recognized (Kay et al., 2017).

Southeastern New England is dominated by the Avalon terrane, a Gondwanan terrane accreted onto composite Laurentia via a west-dipping subduction zone during the latest Silurian-Devonian Acadian orogeny (Rast et al., 1993; Robinson et al., 1998). A recent model by Hillenbrand et al. (2021) suggests that a high-elevation and low-relief orogenic plateau with greatly thickened crust formed in southern New England during the Acadian orogeny, and that it persisted for about 50 million years. This model is based on thermochronological data, trace element and isotope geochemistry, and monazite petrochronology (Hillenbrand, 2020). Hillenbrand et al. (2021) suggested that the Acadian orogenic plateau may have collapsed after the Acadian orogeny due to the reduced compressional stress associated with the plate reorganization that preceded the collision between composite Laurentia and Gondwana (Robinson et al., 1998). In Nova Scotia, Canada, the Gondwana-derived Meguma terrane was accreted during the Late Devonian Neoacadian orogeny, but there is no evidence for the presence of Meguma in southern New England. The southeasternmost tip of Massachusetts and adjacent offshore regions, southeast of the Nauset magnetic anomaly, have previously been interpreted as part of the Meguma terrane, based on seismic reflection, gravity and magnetic surveys, and K-Ar dates (e.g., Hutchinson et al., 1988; Stewart et al., 1991; van Staal et al., 2009; White et al., 2010). However, Ediacaran granite below the southeasternmost tip of Massachusetts (Leo et al., 1993) is not necessarily indicative of the Meguma terrane, because rocks of the Meguma terrane in Nova Scotia are no older than Cambrian. While it is possible that the granite below the southeasternmost tip of Massachusetts represents basement to the Meguma terrane, it is also plausible that it is part of the Avalon terrane, or perhaps of a northwest African crustal block, as is present below the Georges Bank, 143 km east-southeast of Nantucket, Massachusetts (Kuiper, 2018; Kuiper et al., 2017).

The Appalachian orogenic cycle culminated in the Late Mississippian to Permian Alleghenian orogeny, which involved continent-continent collision of composite Laurentia with Gondwana and the formation of the supercontinent Pangea (Sacks & Secor, 1990; Hatcher, 2002, 2010). The subduction polarity during the final closure of the Rheic Ocean and the formation of Pangea has been debated (e.g., Domeier & Torsvik, 2014). Some studies (e.g., Hermes & Murray, 1988; Nance & Linnemann, 2008; Michard et al., 2010; Nance et al., 2012) suggest that Laurentia was the down-going lower plate during the collision based on the absence of arc-related Carboniferous igneous rocks in the northern Appalachian orogen and the presence of Carboniferous magmatism in Morocco. Conversely, evidence for Permian plutonism in the German Bank (Pe-Piper et al., 2010) and Devonian subduction-related magmatic activity in the Meguma terrane (van Staal

et al., 2009) suggest that Laurentia might have been the upper plate during pre- and/or syn-Alleghanian convergence, or perhaps that the subduction polarity during the closure of Rheic Ocean might have been west-dipping for some period of time.

Approximately 100 million years after its final assembly, Pangea rifted apart and broke up during the Mesozoic (Frizon de Lamotte et al., 2015). The Hartford basin in the central part of southern New England is one of the abandoned rift basins created during Mesozoic rifting and continental breakup (Hubert et al., 1992; Withjack & Schlische, 2005; Withjack et al., 2002). This basin is an asymmetrical half-graben bounded on the east by the Eastern Border Fault system (Hubert et al., 1992). The preexisting bedrock geology beneath the Hartford Basin was overprinted by the sediments that filled in the basin. The sedimentary units of the basin are thought to be about 5–8 km thick, based on the structural offset and the displacement of isograds (Robinson et al., 1989) and on seismic refraction data (Wenk, 1984).

1.2. Receiver Function Studies on Crustal and Mantle Structure

Receiver function analysis is based on identifying seismic waves that are converted at structural discontinuities with seismic impedance contrasts caused by changes in material properties (Langston, 1979; Rondenay, 2009). Converted waveforms provide information on the amplitude of impedance contrast across the discontinuity, the distance over which the change occurs (the sharpness of the discontinuity), and the depth of the discontinuity (Levin et al., 2016; Rondenay, 2009; Rychert et al., 2007). The seismic impedance is controlled by both the density and seismic velocities of the material, which are often positively correlated in the Earth (Birch, 1961). Synthetic analysis shows that the amplitudes of both P wave to S wave conversions (Ps) and S wave to P wave conversions (Sp) are mostly dependent on the S wave velocity contrast (e.g., Rychert et al., 2007). Therefore, discontinuities imaged by receiver function studies in most cases mainly reflect the change of the effective S wave velocity across the interface, either through changes of isotropic material properties or via the presence of anisotropy.

A number of receiver function studies, using both Ps and Sp phases, have been conducted throughout eastern North America (e.g., Hopper & Fischer, 2018; Levin et al., 2017; Li et al., 2018, 2020), including regional studies focused on specific lithospheric features associated with past tectonic events (e.g., Hopper et al., 2017; Long et al., 2019; Parker Jr. et al., 2013). Ps receiver functions can be used to characterize the thickness of the crust, as well as to resolve detailed structural variations within the crust and shallow mantle lithosphere. The higher frequency content in recordings of Ps phases provide better resolution than Sp receiver functions, although this method is susceptible to multiple reflections from shallower discontinuities that can obscure deeper discontinuities (Rondenay, 2009; Rychert et al., 2007). Recent examples of Ps receiver function imaging of lithospheric structure beneath eastern North America include work by Long et al. (2019), who identified the likely deformation front of Grenville orogeny as an east-dipping, radially anisotropic shear zone within the crust. Additionally, Levin et al. (2017) conducted Ps receiver function analysis to study properties of the Moho discontinuity beneath a long seismic profile crossing the Superior craton, Grenville Province, and Appalachian domains. They found that the Moho discontinuity is deeper beneath the Grenville Province and shallower beneath the Superior craton, while Appalachian domains also have overall thin crust but with more variations. Based on data from the Earthscope Transportable Array (IRIS Transportable Array, 2003), Li et al. (2018) found that the change in Moho depth across the Appalachian front is particularly dramatic in southern New England, implying that the origin of the offset may be more complicated than a simple preexisting crustal thickness difference. To probe deeper features, Sp receiver function analysis is often used, because this analysis is less susceptible to interference from multiple phases (e.g., Vinnik et al., 2004). Like Ps receiver function analysis, it has been used to probe structures beneath eastern North America, principally to characterize the base of the lithosphere (e.g., Hopper & Fischer, 2018). Sp receiver function analysis also proved useful to image structures within the crust like the Suwannee suture beneath the southern Appalachians (Hopper et al., 2017).

1.3. Goals of This Study

In this study, we report a high-resolution seismic discontinuity survey using Ps receiver function analysis based on data from the Seismic Experiment for Imaging Structure beneath Connecticut (SEISConn). We

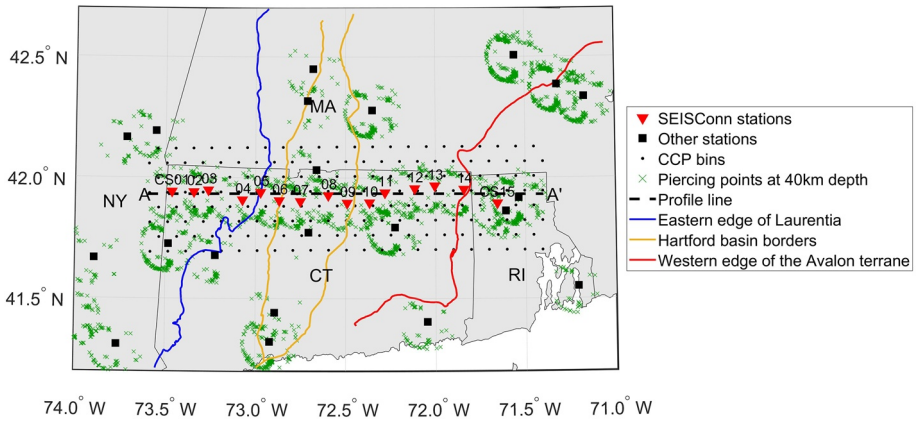

Figure 2. Map of seismic stations used in this study. Red triangles denote Seismic Experiment for Imaging Structure beneath Connecticut stations, which are numbered from CS01 to CS15 from west to east. The black dots denote geographic locations of 0.1° radius bins where receiver functions are stacked to produce the common conversion point (CCP) profile shown in Figure 7, and the black broken line is the profile line. Black squares denote other seismic stations that provide data to the Global Lithospheric Imaging with Earthquake Recordings (GLImER), and that may contribute to our CCP stacking. Theoretical conversion points of Ps phases at 40 km depth are plotted as green crosses. Colored lines show the eastern edge of Laurentia (blue), the boundaries of the Hartford Mesozoic rift basin (yellow), and the western edge of the Avalon terrane (red).

provide a detailed view of the lithospheric structures beneath southern New England to understand the geometrical relationships between structures imaged at depth and the complex surface bedrock geology (Figure 1). The overarching goal of our seismic imaging is to shed light on the lithospheric expression of fundamental plate tectonic processes that have operated beneath southern New England in the past, and to use our images to illuminate the complex tectonic history of the region.

2. Data and Methods

2.1. The Seismic Experiment for Imaging Structure Beneath Connecticut (SEISConn)

The SEISConn deployment (Long & Aragon, 2020) consisted of 15 seismic stations (CS01-CS15 from west to east) deployed in a linear array with ~150 km aperture and ~11 km station spacing (Figure 2). SEISConn stations were deployed between 2015 and 2019. Trillium 120PA broadband seismometers and Taurus digitizer/dataloggers were used, recording data at 40 Hz sample rate on three broadband channels oriented in the east, north, and vertical directions. The SEISConn array traverses a variety of geologic features and major terrane boundaries (Figure 2). CS04 and CS05 are on the boundary between Laurentia and Moretown terrane accreted during the Taconic orogeny; CS14 is on the boundary between Ordovician arc rocks and Avalon terrane accreted during the Acadian orogeny; CS07 to CS09 were deployed within the Mesozoic Hartford rift basin. In addition to the SEISConn stations, we also incorporate data from the Transportable Array, the New England Seismic Network, and the Lamont-Doherty Cooperative Seismic Network to produce our common conversion point (CCP) images (Figures 7 and 8).

2.2. Ps Receiver Function Methodology

For Ps receiver function analysis, the incident waves used are typically teleseismic direct P waves (Langston, 1979; Rondenay, 2009; Rondenay et al., 2017; Rychert et al., 2005). We followed the procedures laid out by Rondenay et al. (2017) and selected earthquakes with magnitudes larger than 5.5, at epicentral distances between 29° and 98°. Earthquakes at shorter epicentral distances will have less vertical P wave incidence and may include P waves that are triplicated by the mantle transition zone, while ones at larger epicentral distance will have P waves diffracted along the core-mantle boundary instead of a direct arrival. The selected data were down-sampled to 10 Hz, band-passed filtered with corner frequencies of 0.03 and 4.9 Hz, and then rotated to the vertical-radial-transverse (Z-R-T) coordinate system, in which the incident P phase

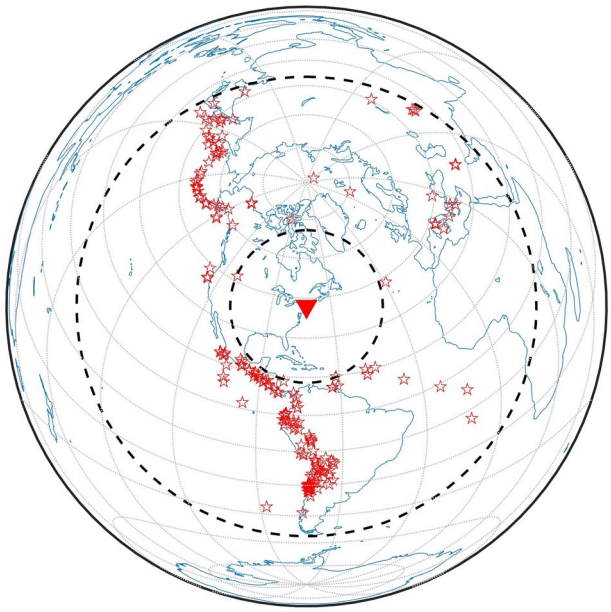

Figure 3. Map of earthquakes used in this study. Red triangle is the location of the Seismic Experiment for Imaging Structure beneath Connecticut array. Black dashed lines denote the epicentral distance limits of 29° and 98°. Red stars denote earthquakes for which the data pass the quality control process before calculating receiver functions.

and the converted S phase are mostly recorded on Z and R components, respectively.

A minimum magnitude of 5.5 does not guarantee a high signal-to-noise ratio (SNR) at teleseismic distances, so we implemented a set of quality control processes to select high-quality waveforms. Signal windows used for the main pulse and the coda were 0–7.5 s and 15–22.5 s after the onset of the incident P wave, respectively. The noise window used was 5–22.5 s before the onset of the incident P wave. Only traces with SNR larger than 10 on the Z component and 8.8 on the R component were retained for further analysis. Also, traces with codas larger than main pulses were excluded to enhance the stability of the deconvolution. Figure 3 shows the distribution map of events which passed the quality control procedure for at least one station. Next, we deconvolved the components to remove the effect of the source-time function and the instrument response, and highlight the impulse response of the structures beneath the station contained in the converted S phase. There are several established ways to carry out this deconvolution in either the time domain or frequency domain (Rondenay, 2009). In this study, we make use of multiple deconvolution methods.

First, we calculated single-station receiver function stacks using FuncLab, a MATLAB program for receiver function analysis (Eagar & Fouch, 2012; Porritt & Miller, 2018). FuncLab implements an iterative, time-domain deconvolution method, as applied by Ligorría and Ammon (1999). During each iteration, the R component is cross-correlated with the Z component to add a new spike to the receiver function estimate, which is then convolved with the Z component and subtracted from the R component. As a result, the convolution of the receiver function estimate with Z component becomes closer to the original R component after each iteration; the receiver function estimate therefore becomes closer to the true response of the structure beneath the station. The iterative process was stopped when either maximum number of iterations was reached (we allowed 200) or the change to the misfit by further iterations became trivial (less than 0.001%). A low-pass Gaussian filter with a width of 2.5 was applied to suppress high-frequency noise in the receiver function. The calculated receiver functions were automatically quality controlled by FuncLab to exclude traces with larger than 20% misfit, and the remaining traces were visually inspected to exclude ones with unusually large pre-arrival noise. The selected receiver functions were then migrated from the time domain to depth using the IASP91 global one-dimensional (1-D) velocity model (Kennett & Engdahl, 1991) and stacked by station after a moveout correction based on calculated ray parameters.

Next, we generated CCP stacked images in the framework of the Global Lithospheric Imaging with Earthquake Recordings (GLImER) system (Rondenay et al., 2017; Sawade, 2018). The traces were further rotated from Z-R-T into L-Q-T coordinate system, which minimizes the P wave energy in components other than L by estimating the incident angle of P wave. GLImER implements a frequency domain deconvolution scheme. The receiver functions were computed by least squares inversion with spectral division of the Fourier transformed Q-component by the Fourier transformed L-component, and multiplication of both numerator and denominator by the complex conjugate of the L-component. This spectral division is stabilized with a regularization parameter based on pre-event noise levels, which minimizes large amplification at discrete frequencies (i.e., ringing artifacts) in the resulting receiver function. Computed receiver functions were mapped to depth by ray tracing and computing Ps delay times through a simplified version (horizontal layer equivalent—i.e., 1-D model along the ray) of the three-dimensional global GyPSuM velocity model of Simmons et al. (2010). These computations were done for a spherical earth, with corrections for surface topography. Owing to the dense spacing of SEISConn and neighboring stations, the resulting receiver functions can be grouped and stacked according to common conversion points (CCP bins) at depth. Stacking receiver functions at CCP bins allows us to construct an image with improved lateral and depth resolution compared to single stations analysis (e.g., Rondenay, 2009). We used staggered circular CCP bins with 0.1°

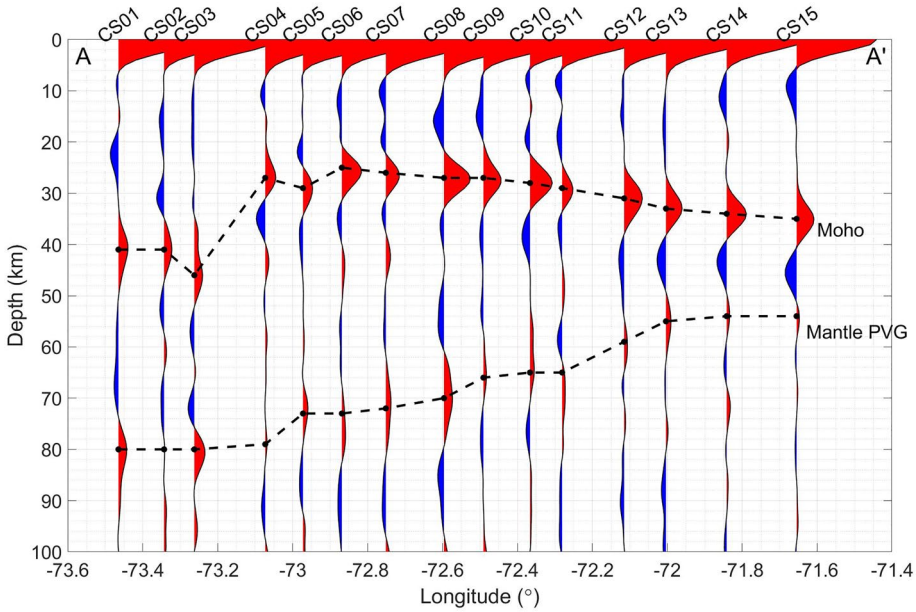

Figure 4. Single-station stacked receiver function profile beneath Seismic Experiment for Imaging Structure beneath Connecticut (SEISConn) stations. We show stacked radial component receiver functions for each SEISConn station, from CS01 in the west to CS15 in the east. Data are band-passed between 0.2 and 2 Hz. Positive (red) pulses indicate positive velocity gradient (PVG) where the seismic velocity is increasing with depth and negative (blue) pulses indicate negative velocity gradient (NVG) where the velocity is decreasing with depth. Larger-amplitude pulses suggest greater velocity contrasts. The inferred Moho discontinuity and a west-dipping positive discontinuity in the lithospheric mantle are shown with dashed lines.

spacing (black dots in Figure 2) and a maximum overlap of 27% of the bin radius. Binning with depth is done at 2-km increments, generating a CCP volume through which cross-sections can be extracted for visualization. Here, we present the west-east profile shown as the black line in Figure 2.

3. Results

3.1. Single-Station Results

Figure 4 shows Ps receiver function single-station stacking image plotted with data band-passed between 0.2 and 2 Hz. The most prominent feature is the Moho discontinuity, a positive velocity gradient (PVG) whose timing suggests an interface at ~42 km beneath the western part of the array, at ~27 km beneath the central part, and at ~35 km beneath the eastern part. With very compact station spacing of SEISConn array, we are able to constrain the change of Moho depths across the edge of Laurentia in the western part of the array with higher resolution than has been possible in previous studies (e.g., Li et al., 2018, 2020). The Moho shallows by 15 km over a horizontal distance of about 20 km from west to east between station CS03 and CS04, and then gradually deepens to the east in a smooth fashion across the rest of the array. The other prominent feature in this image is a PVG beneath the Moho, in the lithospheric mantle, that is visible on the stacks for nearly every station. The depth of this PVG gradually increases from east to west, from ~55 to –80 km. The lateral coherence of this PVG along the array suggest the presence of a west-dipping discontinuity in the lithospheric mantle beneath the SEISConn line. In addition to these major features, the presence of other possible converters both within the crust and within the lithospheric mantle are suggested by the single-station stacks, but are not well-resolved by this method.

We also carried out single-station stacking with different frequency contents to evaluate the sharpness of the interfaces that are revealed by the single-station receiver function analysis (Figure 5). We first raised the minimum frequency of the data to 0.5 Hz (implementing a bandpass between 0.5 and 2 Hz), as shown in Figure 5a; this image includes less long-period energy than the image shown in Figure 4. With this frequency content, the Moho signals to the west of the Moho step are significantly attenuated, while those to the

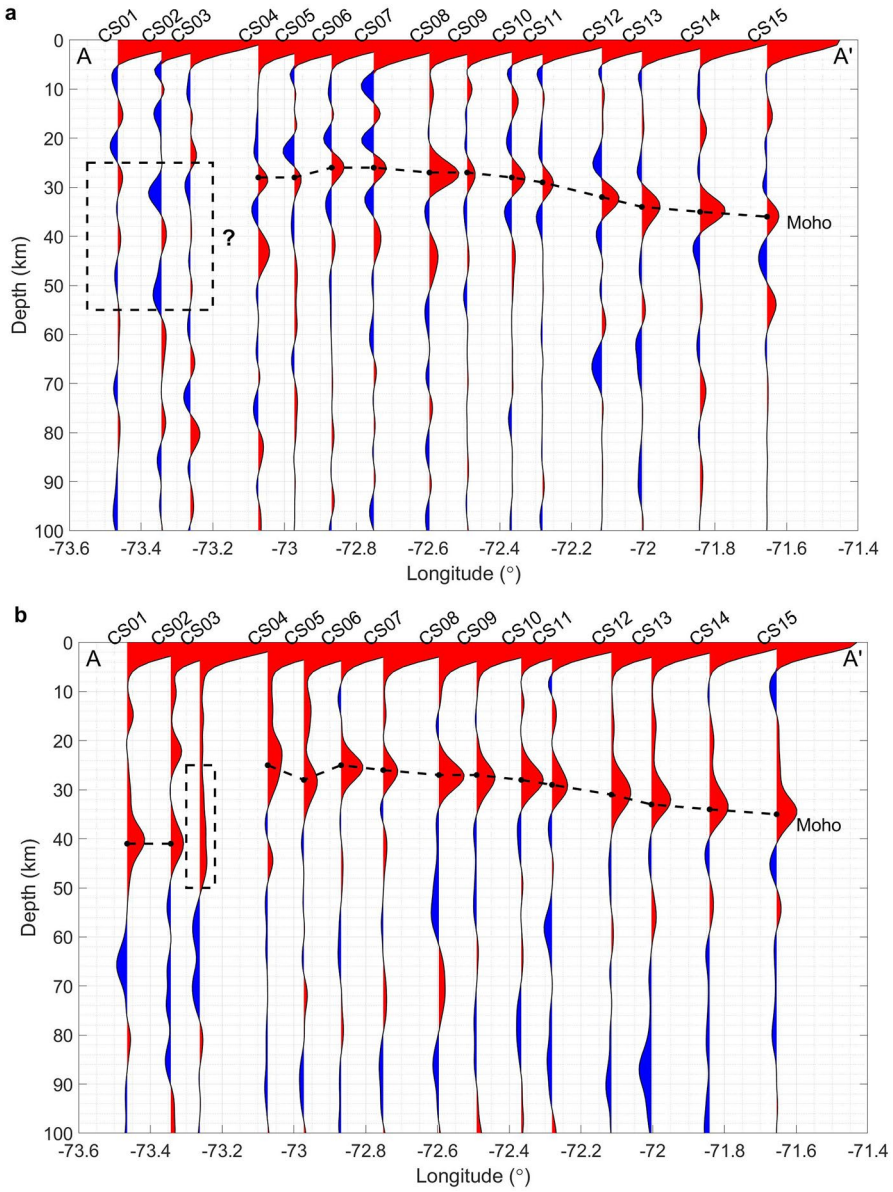

Figure 5. The single-station stacking profile of Seismic Experiment for Imaging Structure beneath Connecticut array plotted with different frequency contents. Color conventions are as in Figure 4. (a) Data are band-passed between 0.5 to 2.0 Hz, including less low frequency signal compared with Figure 4. The black dashed rectangle highlights diminished Moho signals beneath CS01 to CS03. (b) Data are band-passed between 0.03 to 1.5 Hz, the same frequency band as common conversion point images (Figures 7 and 8), including more low frequency signal compared with Figure 4. The black dashed rectangle highlights the more spread Moho signal beneath CS03.

east of the Moho step remain strong. This observation (that the Moho to the west of the step is not clearly observed when high-frequency data is emphasized) suggests that the transition from the seismic velocity in the crust to that in the mantle occurs over a larger vertical distance, and therefore that the Moho is less sharp, to the west of the Moho step. Also, the west-dipping PVG in the lithospheric mantle is less prominent in this frequency band, which means that the velocity gradient across this mantle PVG is overall weaker than the gradient across the Moho beneath these accreted terranes. On the other hand, after lowering the minimum frequency of the data to 0.03 Hz (implementing a bandpass between 0.03 and 1.5 Hz), and therefore including more long-period energy, we find that receiver functions stacked at station CS03, located near the Moho step, no longer exhibit a well-defined Moho conversion, as shown in Figure 5b. Instead, the signals of Ps phases converted at the Moho signals seem to spread over a wide range of depths.

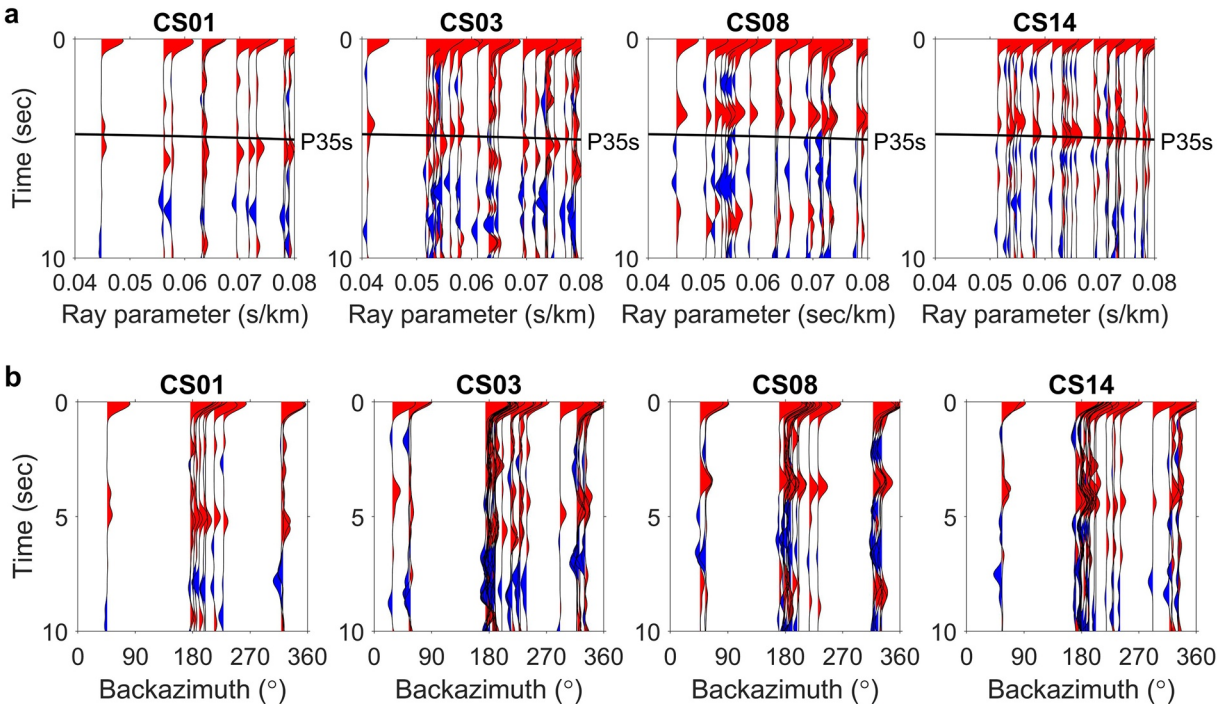

Figure 6. (a) Ray parameter gathers and (b) Backazimuth gathers for four example Seismic Experiment for Imaging Structure beneath Connecticut stations (CS01, CS03, CS08, and CS14, as shown on each plot). Data are band-passed between 0.03 and 1.5 Hz. Color conventions are as in Figure 4. For each station, individual receiver functions traces (migrated to depth) are plotted as a function of ray parameter (top panels) or event backazimuth (bottom panels). Black lines on ray parameter gathers show expected moveout of Moho signals from a 35 km deep Moho, predicted using the IASP91 1-D velocity model (Kennett & Engdahl, 1991).

In order to gain further insight into the complexity of the discontinuities revealed by our data, and to investigate possible contamination by multiple reflections, we also computed single-station receiver function gathers as a function of ray parameter and backazimuth for SEISConn stations. Examples of these gathers for four representative stations (CS01, CS03, CS08, and CS14) are shown in Figure 6. At all four example stations, the Moho is observed across all backazimuths and ray parameters, but the data at station CS03 show unusual variations of Moho depths in comparison with those at stations far away from the Moho step (CS01, CS08, and CS14). The Moho signal at CS03 exhibits a distinct backazimuthal dependence, where events arriving from the north show multiple Ps arrivals (at 6 s as well as at around 3–4 s), while those arriving from the south show a more uniform Moho Ps signal at ~4 s. Receiver functions at other stations have more consistent Moho signals regardless of event back azimuth; however, all stations exhibit some complexity in the arrival of intracrustal and/or intralithospheric converted phases with respect to backazimuth and/or ray parameter. This behavior suggests that there may be relatively complex structures within the crust and/or mantle lithosphere that are obscured by the approach of stacking receiver functions over all backazimuths and ray parameters, as was done in Figures 4 and 5.

3.2. CCP Image Results

Figure 7 shows our CCP profile produced in the GLImER framework, with data band-passed between 0.03 and 1.5 Hz. Due to the different frequency content and different stacking conventions, although the first-order features of the CCP profile resemble those of the single single-station stacked image in Figure 4, the CCP profile displays more robust features. Furthermore, since the traces are rotated to L-Q-T coordinate system to produce the CCP profile, P to S conversions at relatively shallow depths (as shallow as ~5 km) can be distinguished, whereas they are generally overprinted by the direct P arrival and its sidelobes in the single-stack image (Figure 4). Figure 7 is produced by stacking traces within each 0.1° radius CCP bin, interpolated to 200 cells per degree.

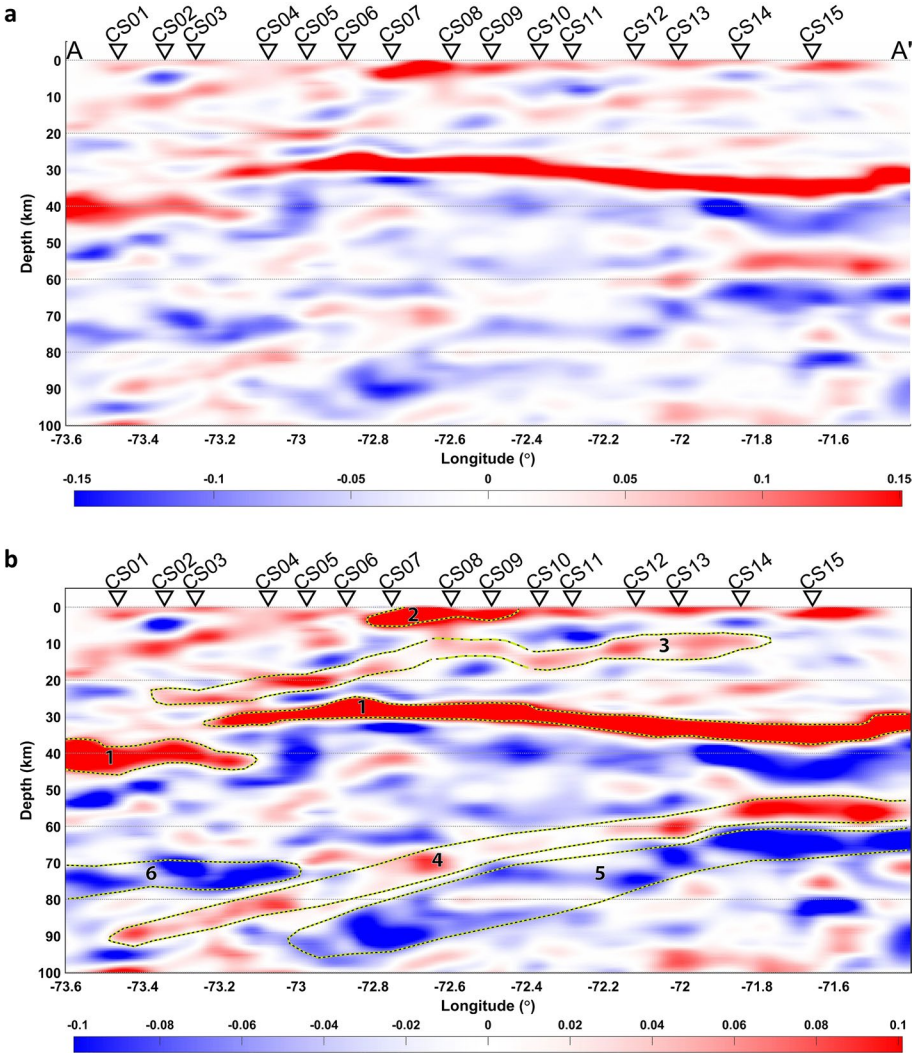

Figure 7. (a) Common conversion point (CCP) profile beneath the Seismic Experiment for Imaging Structure beneath Connecticut (SEISConn) array (section line A-A′ is shown on Figure 2). Profile was constructed by stacking Q component receiver functions at each CCP bin with 0.1° radius, interpolated to 200 cells per degree. Black triangles show the locations of SEISConn stations, from CS01 in the west to CS15 in the east. Red (positive) colors indicate that the seismic velocity increases with depth; and blue (negative) colors indicate that the velocity decreases with depth. Color scale shows the amplitude of the converted wave as a fraction of P wave amplitude, with deeper colors suggesting greater velocity contrasts. (b) Same CCP profile with discussed features contoured and numbered. We use a slightly narrower color bar than in (a) to accentuate features.

Here, we observe a number of prominent and robust features within both the crust and mantle lithosphere. We see a strong Moho converter whose geometry includes a step-like feature in the western portion of the array, with a suggestion of a doubling of Moho near the step, as well as a shallow Moho in the central part of the array (~27 km) and a gradual deepening to the east (feature #1 in Figure 7b). Next, we observe a strong and shallow PVG beneath SEISConn stations CS07–CS09 at about 5 km depth (feature #2 in Figure 7b). We also observe evidence of deeper discontinuities within the crust; the most prominent of these is a west-dipping PVG located ~10 km beneath station CS14 in the east and ~25 km beneath station CS02 in the west (feature #3 in Figure 7b). The PVG appears to shallow in the central part of the profile, suggesting that it may not be a single, continuous feature.

Beneath the Moho, there is evidence for several discontinuities within or near the base of the mantle lithosphere. These include a prominent west-dipping PVG (feature #4 in Figure 7b), which is also noticeable on the single-station stacks (Figure 4). This feature appears at a depth of ~55 km in the eastern part of the

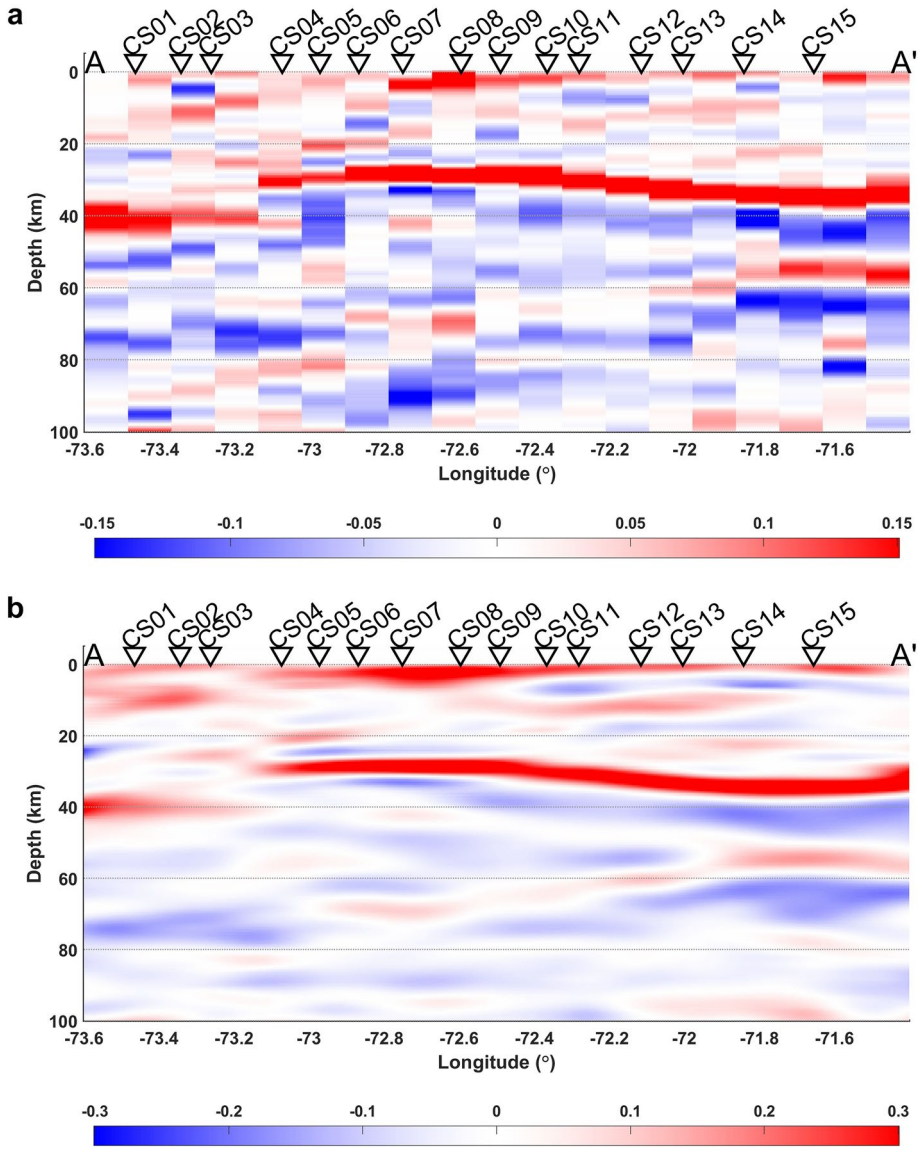

Figure 8. The Common conversion point (CCP) profile of the Seismic Experiment for Imaging Structure beneath Connecticut array plotted with less horizontal interpolation and with larger bin size. Color conventions are as in Figure 6. (a) The CCP profile with 0.1° radius CCP bin, interpolated to 10 cells per degree. (b) The CCP profile with 0.2° radius CCP bin, interpolated to 200 cells per degree. The color bar ranged is doubled for doubled data coverage radius at each bin.

array and at a depth of ~90 km beneath the western part of the study area. In addition to the prominent PVG, the CCP image also clearly shows three negative velocity gradient (NVG) features. The first is a NVG located beneath the Moho. Another NVG (feature #5 in Figure 7b) is located beneath the west-dipping lithospheric PVG described above. The NVG has a similar geometry to the overlying PVG, but it is not identical. This west-dipping NVG is ~65 km beneath the eastern end of the array and the depth increases to ~90 km beneath the stations CS05 and CS06 in the west. There is another nearly horizontal NVG at a depth of ~75 km beneath the western portion of the array (feature #6 in Figure 7b). Due to the large and sharp velocity contrast across the Moho, we must consider that this large positive converted signal can have noticeable negative sidelobes with amplitudes comparable to the signals from weaker discontinuities (e.g., Rychert et al., 2018). Therefore, the NVG that appears directly beneath the Moho is likely to be a sidelobe of the Moho conversion, instead of an interpretable feature. On the other hand, the west-dipping PVG (feature #4 in Figure 7b) and NVG (feature #5 in Figure 7b) that appear at lithospheric mantle depths have similar

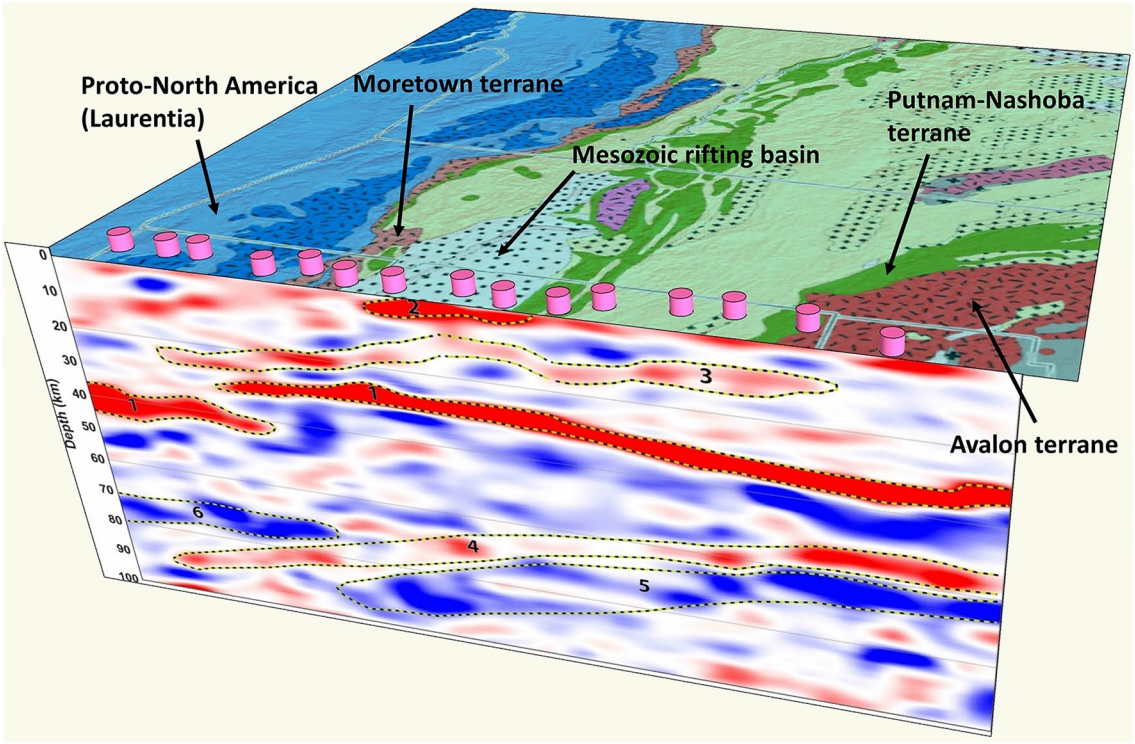

Figure 9. Block diagram that shows our common conversion point (CCP) image (Figure 7b) beneath bedrock geologic features (Figure 1). Interpretable features of the CCP image referred to in the text are marked. Feature #1 is the step-like change of Moho beneath the boundary between the Grenville province of Laurentia and terranes accreted during Taconic orogeny (including the Moretown terrane). Feature #2 is the strong positive velocity gradient (PVG) beneath Hartford basin. Feature #3 is the west-dipping PVG feature(s) in the crust. Feature #4 is the west-dipping PVG converter in the lithospheric mantle. Feature #5 is the west-dipping negative velocity gradient (NVG) converter in the mantle, which may connect to feature #6, the flat-lying NVG feature beneath the western portion of the array. Station locations shown by pink cylinders.

amplitudes and their geometries are not identical. Therefore, neither is likely to correspond to an imaging artifact of the other. Furthermore, the geometries of these two west-dipping, mid-lithosphere converters are very different from that of the Moho, so they are not multiple reflections from the Moho either; rather, these features likely correspond to physical discontinuities within the mantle lithosphere. Similarly, the flat-lying NVG (feature #6 in Figure 7b) at ~75 km depth beneath the western part of the array appears to correspond to a physical discontinuity and is not easily explained as an imaging artifact.

To determine the reliability of features in the CCP profile found in Figure 7, we also generated CCP profiles with different bin size and smoothing conventions, testing whether the features that we identify as robust and interpretable persist in the images when different stacking and plotting conventions are used. Figure 8a shows a CCP profile with less horizontal interpolation (that is, with less smoothing), and Figure 8b shows one generated using a larger bin size (therefore, greater horizontal averaging). This allows us to assess whether major features persist when less smoothing is applied, or when more horizontal averaging is used. Although the images in Figures 7 and 8 are different, the major features that we interpret as physical discontinuities are present regardless of the bin size or smoothing conventions used. Thus, these features are not likely to be imaging artifacts introduced by plotting conventions.

4. Discussion

In the following, we focus on exploring possible explanations or models for the major features of the single-station stacks (Figure 4) and the CCP image (Figure 7) that are discussed in Section 3 above. Our interpretation focuses on features that display relatively large amplitudes in the receiver function images, and/or are observed continuously across portions of the image using data from multiple stations. Features with relatively small amplitudes, of limited spatial extent, and/or that are only observed at a single station are

more likely to be imaging artifacts, and we do not include these features in our discussion. In order to place our receiver function results in a geologic and tectonic context, in Figure 9 we show a 3D block diagram that joins the SEISConn CCP profile (Figure 7) with the surface bedrock geology map (Figure 1). In Figure 9, we highlight the major features of the CCP image that have potentially important implications for our understanding of the tectonic history of southern New England. These include the Moho, particularly the Moho step (feature #1 in Figure 9) beneath the eastern margin of Laurentia, the relatively shallow PVG beneath Hartford basin (#2), the west-dipping PVG feature(s) in the crust (#3), the west-dipping PVG at mantle depths (#4), and the west-dipping NVG lying beneath it (#5), which may be connected to the flat-lying NVG at ~75 km depth in the western part of the array (#6). Most of these features do not have one definitive interpretation, since seismological evidence presented in this study only provide a snapshot of current structure with no temporal information. We discuss and explore all reasonable interpretations based on locations and geometries of these features, in combination with the geologic background and tectonic history.

4.1. Crustal Thickness and the Moho Step

The Moho is the most prominent and robust discontinuity imaged in this study. Key features include relatively thick crust in the western portion of the array, a step-like change in Moho depth moving to the east, thin crust beneath the central part of the study area, and a gradual deepening of the Moho at the eastern end of the array (Figure 9). The step-like change of the Moho depth (feature #1 in Figure 9) is unambiguously imaged by our analysis, and is clear in both the single station stacking profile (Figure 4) and the CCP profile (Figure 7). The observed Moho depth variations beneath SEISConn are consistent with a larger-scale receiver function study based on the EarthScope Transportable Array (Li et al., 2018). Our much denser station spacing allows for more detailed imaging of variations and shows that the change in Moho depth across the step occurs over a shorter length scale (~20 km) than is possible to image using the Transportable Array data (~70 km station spacing) alone. As pointed out by Li et al. (2018), the change in Moho depth in southwestern New England spatially correlates with a Bouguer gravity anomaly variation (Bonvalot et al., 2012), but does not coincide with a topographic gradient. The Moho step in our CCP image is located in the vicinity of the boundary between the Laurentian rifted margin to the west and the Gondwana-derived Moretown terrane, accreted during the Ordovician Taconic orogeny, to the east. Therefore, this Moho depth offset is likely to be the manifestation of the Grenville-Moretown terrane boundary at depth (Li et al., 2018, 2020). Here we consider three possible models for the formation and preservation of the Moho step: (a) the step represents the juxtaposition, during the Taconic orogeny, of crustal blocks with preexisting differences in thickness and composition, (b) the step was formed via underthrusting of Laurentia during the Taconic orogeny, or (c) the step was formed after the Taconic orogeny by younger tectonic events. Regardless of the details of its formation, it is likely that the Moho step has persisted over several hundred million years, suggesting that the thicker crust on the west side of the step is particularly strong.

It is possible, and perhaps likely, that the Laurentian rocks west of the step and Gondwana-derived terranes to the east had intrinsically different crustal properties before they were juxtaposed during the Taconic and later orogenies. The Grenville orogenic belt of Laurentia was formed during earlier collisional events that culminated in the assembly of the supercontinent Rodinia (e.g., Li et al., 2008). The ratio of P wave velocity to S wave velocity (V_p / V_s) in the Grenville crust has been shown to be larger than that in the crust of accreted terranes, implying a generally more mafic Grenville crust (Levin et al., 2017; Musacchio et al., 1997). Instead of assuming a uniform V_p / V_s ratio as in 1-D velocity models, if an averaged V_p / V_s ratio of 1.81 is used for the Grenville crust and 1.73 is used for the crust of accreted terranes (Musacchio et al., 1997), the observed ~15 km Moho depth offset at the Grenville-Moretown terrane boundary would be reduced to ~12 km. Although the uncertainty involved by V_p / V_s variations can by no means fully explain the observed step-like change of Moho depth, it can partially contribute to the large size of the Moho step. Even with varying V_p / V_s ratios considered, the Grenville crust is still thicker than the crust of the Appalachian in general (Levin et al., 2017). Thickened crust beneath the Grenville orogenic belt has been attributed to mafic magmatic underplating, which would result in a more gradational Moho (Petrescu et al., 2016). Such a gradational Moho is consistent with our single-station stacking observations using high-frequency data at SEISConn stations located to the west of the Moho step (Figure 5a). One possible model for the Moho step, then, explains the observed drastic offset of the Moho simply in terms of preexisting differences in the V_p / V_s ratio and the thickness of the Grenville crust and those of the Moretown terrane to the east.

Preexisting differences in crustal properties can also account for observed smaller than expected gravity anomaly increase across the Moho step. If east and west sides of the Moho step have same crust and mantle densities, a 15 km difference in crustal thickness would produce ~250 mGal Bouguer gravity anomaly difference. However, the observed Bouguer anomaly increase across the Moho step is only ~120 mGal (Bonvalot et al., 2012; Li et al., 2018). A more mafic and thus denser Grenville crust can result in a smaller than observed Moho step as well as a smaller than expected Bouguer gravity anomaly change across the Moho step. Furthermore, potentially thicker lithospheric mantle beneath Laurentia, which will be discussed in detail later, can also contribute to a smaller gravity increase across the Moho step.

Another possibility invokes processes involved with Moretown terrane accretion, in addition to preexisting differences in crustal thickness, as a contributing cause of the Moho step. When the Moretown terrane was accreted to Laurentia during the Taconic orogeny, the subduction zone was likely east-dipping, with the Moretown terrane on the hanging wall of the thrust (Karabinos et al., 2017; Macdonald et al., 2014). Therefore, it is possible that the Laurentian crust was underthrust below the Moretown terrane crust (and the top of its mantle lithosphere) to the east during terrane accretion. The abrupt cutoff of the Laurentian Moho at the Moho step is consistent with slab breakoff during the terrane accretion. Later episodes of compressional stress during subsequent phases of Appalachian orogenesis (the Acadian and Alleghenian orogenies) may have reactivated and further increased the extent of this underthrust structure. Such an underthrust could potentially explain why the Moho seems to be doubled between the stations CS03 and CS04 in CCP images (Figures 7 and 8). The phenomenon of a double Moho is observed in both active tectonic zones like Tibet and ancient orogens like the Appalachians, and it is typically interpreted either as reflecting lower crustal layering (e.g., Benoit et al., 2014) or as a result of thrusting at the terrane boundary (e.g., Kind et al., 2002; Wagner et al., 2012). Beneath SEISConn, the double Moho accompanies the step-like change of Moho depths across the Grenville-Appalachian terrane boundary and is therefore likely to be associated with the accretional geometry. In this framework, the deeper discontinuity would correspond to the bottom of the Laurentian crust, the footwall of the thrust, and the shallower discontinuity would correspond to the Moho of the Moretown terrane. Possible additional support for this model comes from the ray parameter and back azimuth gathers at the station CS03 (Figure 6), which suggest a complicated Moho geometry and display a prominent back-azimuthal dependence in the arrival of the Moho converted pulse. Specifically, P waves arriving from the north are converted to S waves at only one depth (35–40 km), whereas P waves arriving from the south are converted to S waves at depths greater than 40 km, as well as at several shallower depths. Given that the boundary between Laurentian and accreted terranes at this latitude generally trends northeast-southwest (Hatcher, 2010; Hibbard et al., 2006) and that station CS03 is located on the west side of the boundary, rays coming the north/northwest may only sample the crust on the Laurentia side, whereas rays coming from the south/southeast can sample the crustal complexities beneath the terrane boundary. The observation that the Laurentian Moho appears to be deeper on the traces arriving from the south, which sample the structure at the Moho step, suggests a local deepening of the Laurentian Moho at the Moho step, caused by the underthrust of the Laurentian crust during the Taconic orogeny.

A third possible model is that the Moho step was created and/or modified by tectonic events younger than the Taconic orogeny. The large-scale receiver function study of Li et al. (2020), which characterized Moho depths across much of eastern North America, showed that the step-like Moho across the Grenville-Appalachian terrane boundary is not continuous throughout the Appalachians. Instead, it is particularly significant along a portion of the margin that extends from southern New England southward to the central Appalachians. This may imply that the Grenville-Appalachian boundary in this portion of the margin was modified by younger tectonic events, resulting in a more drastic Moho step. Motivated in part by the results of Li et al. (2020), Hillenbrand et al. (2021) suggested that the Moho step can be attributed to the post-Acadian collapse of the Acadian orogenic plateau. Thermobarometric analysis of high-pressure granulites from northeastern Connecticut (Keller & Ague, 2018), as well as compilations of the trace element and isotope geochemistry of syn-Acadian igneous rocks (Hillenbrand, 2020), suggest that the crust during and after the Devonian Acadian orogeny, referred to as the Acadian altiplano by Hillenbrand et al. (2021), was at least 55 km thick. During the Acadian orogeny, the excess gravitational force from the increased topography of the Acadian altiplano was presumably counterbalanced by the large compressional stress at the convergent boundary. Hillenbrand et al. (2021) proposed that the Acadian altiplano may have collapsed due to reduced compressional stress after the Acadian orogeny as a result of decreased convergence rate or plate

reorganization associated with approach of Gondwana (Robinson et al., 1998). The crust may also have thinned at this time due to channel flow and ductile extrusion of mid-crustal rocks toward the southeast, as has been proposed for the Putnam-Nashoba terrane to the east (Severson, 2020). In this interpretation, the extent of this channel to the west is unknown as it is not exposed. Regardless of the mechanism, the collapse of an orogenic plateau due to reduced stress and gravitational forces can greatly reduce the crustal thickness (Dewey, 1988; Rivers, 2012). In the case of the Acadian altiplano, because of the generally thinner lithosphere beneath the accreted terranes compared with that beneath Laurentia, the isostatic equilibrium may have driven crustal thinning further and resulted in a drastic crustal thickness difference between accreted terranes and Laurentia (Hillenbrand et al., 2021). Given the limited along-strike extent of the proposed Acadian altiplano (Hillenbrand, 2020), the plateau collapse model can potentially explain the Moho depth offset across the Grenville-Appalachian boundary beneath southern New England and the region just to the south, resulting in a more drastic Moho step than in other regions along the Appalachian front.

The present-day configuration of the Moho beneath the SEISConn line may have been further modified by the Mesozoic rifting and breakup of Pangea. Beneath southern New England, the Moho is shallowest beneath the Hartford basin, in the central portion of the SEISConn line; to the east of the basin, it deepens smoothly to the east (Figures 4 and 7). The Moho topography to the east of the step might be largely modified by Mesozoic rifting. The crust beneath rift basins is likely to be thinned more than surrounding regions due to concentrated extension (Bell et al., 1988). It is also possible that overall thinning and extension of Appalachian crust during the breakup of Pangea (e.g., Withjack et al., 2020) smoothed out any preexisting crustal thickness differences between various accreted terranes. This may explain why we do not see dramatic contrasts in Moho depths associated with terrane boundaries east of the Laurentian Moho step (for example, between the Avalon terrane at the eastern end of the SEISConn array and the Putnam-Nashoba terrane to its west). Hillenbrand et al. (2021) considered whether Mesozoic rifting may have played a role in forming the Moho step at the edge of Laurentia as well. They showed that the cooling histories for rocks to the west of the Moho step and that to the east of the step converge between ca. 300 and 280 Ma based on $^{40}Ar/^{39}Ar$ K-feldspar dates; therefore, they propose that the Moho step itself is unrelated to Mesozoic rifting or younger tectonic events.

Interestingly, while there are lateral variations in the depth of the Moho converter across the SEISConn line, the amplitude of the converter appears to be relatively constant across the array (Figures 4 and 7). This finding is somewhat puzzling in light of previous results on the crustal velocity structure beneath SEISConn obtained via full-waveform ambient noise tomography (Gao et al., 2020). The model of Gao et al. (2020) includes a high-velocity region in the lower crust beneath the Hartford Basin, which they attributed to the presence of high-density, high-velocity, likely mafic material in the lower crust, emplaced during the rifting that accompanied the breakup of Pangea, and associated with the Central Atlantic Magmatic Province (CAMP). If the rocks of the lower crust beneath the Hartford Basin are indeed particularly fast, then we would expect the velocity contrast between the lowermost crust and the uppermost mantle to be smaller than elsewhere beneath the SEISConn array, leading to lower-amplitude Ps conversions at the Moho. However, this expectation is not borne out (Figures 4 and 7), and we do not have a ready explanation for this puzzling observation. One possibility is that the high-velocity crustal material is distributed through the mid-to-lower crust but is not present in the lowermost crust, leading to a more typical velocity contrast at the Moho, but this apparent paradox warrants further investigation.

4.2. The Shallow PVG Beneath the Hartford Basin

The strong, shallow PVG lying directly beneath the Hartford basin (feature #2 in Figure 9) likely corresponds to the interface between the sedimentary rocks in the basin and the crystalline basement rocks beneath. The eastern North American rift basins were opened by extensional faulting during the Mesozoic, allowing sedimentary units to fill them in Withjack et al. (2002). Seismic wave velocities in the sedimentary layers are much lower than those in the crust (e.g., Condie, 2016). Therefore, the interface between the sediments and the crystalline basement beneath is expected to produce strong Ps converted phases; indeed, Ps receiver function analysis is commonly applied to study the geometry of sedimentary basins (Piana Agostinetti et al., 2018; Zheng et al., 2005). Our CCP profile (Figure 7) suggests a thickness of 5–8 km for the

sedimentary basin, which is consistent with estimates derived from the structural offset and displacement of isograds (Robinson et al., 1989), as well as those from seismic refraction data (Wenk, 1984).

4.3. The West-Dipping PVG in the Crust

The elongate PVG in the crust (feature #3 in Figure 9) consists of up to two possible west-dipping structures; it is not entirely clear whether this converter represents a single discontinuity within the crust, or whether it represents multiple features. In the east, the PVG appears at a depth of ∼10 km beneath the boundary between early Paleozoic arc and back-arc rocks of the Putnam-Nashoba terrane (to the west) and the Avalon terrane (to the east). The PVG feature dips gently to the west, and then appears to shallow again slightly, and perhaps ends approximately beneath the eastern border of Hartford basin. Because of its position related to the geologic units at the surface, with its shallowest point near the eastern boundary of the Avalon terrane, this feature likely represents the Acadian suture in the crust. Physically, the suture may correspond either to the Moho of a relict slab that is preserved in the crust, or (more likely) to a shear zone in the crust associated with the accretion of Avalonia. Similar structures were also observed through seismic reflection data beneath the Newfoundland Appalachians (van der Velden et al., 2004). We envision a relatively thin (perhaps ∼5–10 km) crustal shear zone which accommodated large shear-related deformation, allowing for the crystallographic preferred orientation of crustal minerals, causing seismic anisotropy (e.g., Brownlee et al., 2017) that can manifest as a seismic discontinuity in CCP images. Elsewhere in eastern North America, gently dipping mid-crustal discontinuities have been interpreted as representing either the top or the bottom of a radially anisotropic shear zone with a slow axis that is perpendicular to the layer itself (Hopper et al., 2017; Long et al., 2019). If a radially anisotropic shear zone is indeed present in the mid-crust beneath the SEISConn array, the PVG discontinuity we observe could correspond to the top of the shear zone.

The second, western portion of the mid-crustal PVG feature beneath the center of Hartford basin at a depth of ∼12 km and dips to the west, appearing to end at a depth of ∼25 km near the Moho step. One possible explanation for this feature is that it is associated with an episode of west-dipping subduction during either the Taconic orogeny or the Salinic orogeny. Although the Moretown terrane likely accreted via an east-dipping subduction zone, there may have been a subsequent reversal of subduction polarity during the Taconic orogeny (Macdonald et al., 2014; Karabinos et al., 2017). Karabinos et al. (1998) proposed that the 485–470 Ma Shelburne Falls arc to the west of Hartford basin was formed above an east-dipping subduction zone, while the 454–442 Ma Bronson Hill arc to the east was formed above a west-dipping subduction zone. Given the depth and the slope of the western portion of the crustal PVG feature, its projection to the surface approximately aligns with the western boundary of the Bronson Hill arc. Therefore, it is possible that this west-dipping PVG represents the relict Moho of a west-dipping subducting slab during the second stage of Taconic orogeny (after the accretion of the Moretown terrane and the reversal of subduction polarity). Similar to the Acadian suture explanation for the eastern portion of this elongate PVG, the western portion could also be interpreted as a crustal shear zone associated with the accretion of Ganderia. Karabinos et al. (2017) suggested that the Moretown terrane and Ganderia are distinct terranes, and that the boundary between them is buried under Late Ordovician to Early Devonian rocks to the east of the Bronson Hill arc. Recent Sm/Nd isotopic data suggesting a Ganderian affinity of the Nashoba terrane (Kay et al., 2017) conforms with the idea that the Salinic suture should exist somewhere between the Bronson Hill arc and the Nashoba terrane at this latitude. Similarly, a suture suggested by van Staal et al. (2009) and van Staal et al. (2016) separates two sub-terranes (a leading and trailing edge) of Ganderia which were accreted to the Laurentian margin at different times farther north in Maine, New Brunswick and Newfoundland.

Another possibility is that the two dipping PVGs actually represent one continuous feature that has been modified or disrupted since its formation. A possible scenario is that the inferred crustal shear zone that corresponds to the Acadian suture extends across much of Connecticut, and its geometry has been altered or displaced by younger tectonic events. For example, the hypothesized collapse of the Acadian altiplano involving orogen-parallel escape (Hillenbrand et al., 2021; Massey et al., 2017) would have modified the crustal structure, perhaps altering the geometry of the inferred Acadian suture. Since a noticeable change of geometry occurs beneath Hartford basin, where the shear zone appears to shallow locally, we hypothesize that the localized extension during the Mesozoic rifting may have also played a role in altering its geometry. Gao et al. (2020) suggested that significant mafic magmatic underplating may have occurred beneath

Hartford basin associated with the eruption of CAMP magmatism. We speculate that this addition of lower crustal material may have accompanied, and/or played a role in, alteration of the geometry of the crustal shear zone locally beneath Hartford basin.

4.4. The West-Dipping PVG in the Lithospheric Mantle

The PVG converter in the lithospheric mantle expresses itself in receiver functions stacked at every SEISConn station (Figure 4), and it is also well delineated in the CCP profile (feature #4 in Figure 9) as a nearly continuous, west-dipping feature at lithospheric mantle depths that cuts across the entire profile. Given its depth, continuity, and gently dipping geometry, we hypothesize that the converter corresponds to the Moho of a relict slab from a past subduction event; the deeper portion of the slab likely broke off and sank into the deeper mantle, while the shallower part remained stuck in the stiff, highly viscous lithospheric mantle. Since oceanic crust generally starts to undergo transformation to eclogite at >50 km depth (e.g., Wang et al., 2017), and eclogite has seismic velocities more similar to mantle peridotite (e.g., Worthington et al., 2013), the Ps converted signal from an oceanic Moho at depth is expected to be much weaker in amplitude than that from the continental Moho, as observed. It is notable that while we seem to observe the oceanic Moho, we do not observe a corresponding NVG interface above it that represents the top of the oceanic crust. We speculate that the transformation to eclogite may have made the boundary between the oceanic crust and the continental mantle above less prominent. Furthermore, the NVG representing the top of the oceanic crust is observed in some modern subduction zones (e.g., Yuan et al., 2000) but not in others (e.g., Bishop et al., 2017; Li et al., 2000), suggesting that this interface may be generally harder to image even in modern subduction systems. Finally, the relatively thin oceanic crust and the potentially small amplitude of the NVG may mean that conversions at this interface are lost in the sidelobes of the oceanic Moho PVG, and/or do not appear above the noise level.

The position and geometry of the mantle lithospheric PVG converter suggests a west-dipping subduction event that is contemporaneous with, or younger than, the shallower structures that it cuts across. The timing of the subduction event is therefore critically important, as it can potentially inform models for the later stages of Appalachian orogenesis, but difficult to constrain. The converter does not appear to project to any known terrane boundaries, although its geometry to the east of the dense SEISConn line is uncertain. We offer three hypotheses that could explain the lithospheric PVG converter. The first is that it is a relict slab associated with the subduction event that joined Avalonia to composite Laurentia during the Acadian orogeny. In this scenario, the PVG converter in the lithospheric mantle essentially represents the continuation of the mid-crustal PVG converter (feature #3 in Figure 9), which we interpret as likely corresponding to the Acadian suture; however, they are laterally displaced from each other by ~150 km (with the crustal converter located at about 150 km to the west of the projected location of the mantle converter to crustal depths). This scenario would require an explanation for this displacement. One possibility is that the crust and lithospheric mantle were decoupled and laterally displaced during a later orogeny, most likely the Alleghanian orogeny.

A second possibility is that the relict slab in the mantle lithosphere post-dates the Acadian orogeny and is instead associated with the Late Devonian Neoacadian orogeny. The Meguma terrane, which was accreted onto North America during the Neoacadian, is exposed in Nova Scotia, Canada (Figure 1), but it is unlikely to exist at the latitude of southern New England, unless recently discovered fragments of Proterozoic northwest African crust below the Georges Bank (Kuiper et al., 2017) and southern Rhode Island (Kuiper et al., 2021) represent basement of the Meguma terrane. This opens up the intriguing possibility that the Neoacadian orogeny was associated with a subduction event beneath southern New England, even though there is no firm evidence for terrane accretion at this latitude during this time.

This brings us to a third possibility, which is that the relict slab resulted from subduction of the Rheic Ocean leading to the Alleghanian orogeny and the assembly of Pangea. Because of the westward dip of the PVG converter in our images, this would imply west-directed subduction during the Alleghanian orogeny. The subduction polarity at this time is debated (e.g., Domeier & Torsvik, 2014), however. Nance and Linnemann (2008) argued that, at the latitude of southern New England, Laurentia was the lower plate during the closure of Rheic Ocean and the oceanic slab was therefore subducting to the east beneath Gondwana, based on the absence of arc-related Devonian-Mississippian igneous rocks in the Appalachian orogen (Hermes &

Murray, 1988). Pe-Piper et al. (2010) suggested that there was a transition from dominantly southeastward subduction of Rheic Ocean in the southern Appalachians and southern New England (cf. Nance & Linnemann, 2008) to dominantly northwestward subduction at the latitude of the Permian German Bank pluton south of Nova Scotia. They speculate that the transition occurs at the eastern Gulf of Maine, farther to the north than the SEISConn array. In northwest Africa, subduction during the Alleghanian orogeny is interpreted as having been to the east in the Meseta domain of Morocco at the latitude of most of New England, and to the west in the Anti-Atlas domain of Morocco at the latitude of the Georges Bank in Offshore Massachusetts and the Appalachians south of it (e.g., Michard et al., 2010). It may be that the subduction polarity during the closure of the Rheic Ocean was not constant across different latitudes and/or at different periods of time (Karabinos, 1997). The imaged PVG in the lithospheric mantle records the presence of a relict oceanic slab that subducted and broke off during a period of west-directed subduction, perhaps similar to the Alleghanian one inferred by Pe-Piper et al. (2010) and the Neoacadian one inferred by van Staal et al. (2009) in the Appalachians in southeastern Canada. Assuming a typical subduction rate of 5 cm/year, it would require less than 10 million years of west-directed subduction to leave a relict slab matching the size of this west-dipping PVG. While we cannot distinguish among these three possible scenarios to explain the PVG converter in the lithospheric mantle that we image beneath Southern New England, each of the three possible models has important implications for our understanding of the tectonic history of the Appalachians.

4.5. The NVG Features at Mantle Depths

Finally, we consider the origin of the NVG features at mantle depths beneath southern New England in our CCP images. As discussed previously, the NVG directly beneath the present-day Moho is likely to be an imaging artifact, but robust features include the nearly continuous west-dipping NVG converter that lies beneath the west-dipping PVG (feature #5 in Figure 9), as well as a strong, flat NVG at ~75 km depth beneath the western (Laurentian) portion of the array (feature #6 in Figure 9). Our imaging is generally consistent with preliminary findings of Goldhagen et al. (2019), who applied Sp receiver function imaging to SEISConn and other data and who inferred multiple NVG discontinuities beneath the Moho in the study area, with a clear transition in lithospheric structure across the Laurentian margin. We suggest that the west-dipping NVG (feature #5 in Figure 9) may represent the present-day lithosphere-asthenosphere-boundary (LAB). The decrease of seismic velocities at the base of the lithosphere can produce converted phases with negative polarity which are commonly used to identify the LAB in receiver function studies (e.g., Abt et al., 2010; Hopper & Fischer, 2018; Rychert et al., 2005). If feature #4 is interpreted as the oceanic Moho of a relict slab, this west-dipping NVG is theoretically within the oceanic lithosphere. However, since the proposed relic slab has been stuck in the continental lithosphere for at least a couple hundred million years, it should be in thermal equilibrium with the surrounding continental lithosphere (Luo & Korenaga, 2020). If true, the oceanic lithosphere may have become thinner as it heated up, and its bottom may have been assimilated with the bottom of continental lithosphere. Hopper and Fischer (2018) previously conducted Sp receiver function analysis to image the LAB across the United States using data from USArray and other networks. They suggested that the LAB beneath southern New England deepens from ~65 km in the east to ~75 km in the west, approximately consistent with the mantle NVG imaged in the SEISConn profile. However, previous receiver function studies beneath New England (Rychert et al., 2005, 2007) as well as a global surface wave tomography study (Steinberger & Becker, 2018) suggested larger lithospheric thicknesses (87–105 and ~150 km, respectively). Therefore, the possibility that the NVG observed in previous receiver function profiles is an internal structure within a thicker lithosphere cannot be ruled out without further constraints.

If feature #5 in Figure 9 is indeed the base of the lithosphere, then this suggests particularly thin continental lithosphere beneath the eastern part of southern New England. An interesting question is whether this possible thin lithosphere is associated with a prominent low-velocity seismic anomaly in the upper mantle centered beneath central New England, imaged in a number of seismic tomography studies (e.g., Eaton & Frederiksen, 2007; Li et al., 2003; Menke et al., 2016; Tao et al., 2020). This low velocity anomaly, often referred to as the Northern Appalachian Anomaly (NAA), has a narrow column shape at 60–90 km depths and broadens to the west at 120–200 km depths in most models. It is interpreted either as a relict feature from the passage of the Great Meteor hotspot (Eaton & Frederiksen, 2007; Li et al., 2003) or as a modern asthenospheric upwelling (Levin et al., 2018; Menke et al., 2016), perhaps associated with edge-driven convection. Either way, an upper mantle thermal anomaly can erode and ablate the base of the lithosphere,

creating locally thin lithosphere (Tao et al., 2020). It is not well known, however, whether the NAA extends as far south as the SEISConn line, as different tomography models differ in their details. Lopes et al. (2020) suggested that upper mantle upwelling associated with the NAA may extend as far south as the SEISConn line, at least in the eastern portion of the array, based on the observation of small SKS splitting delay times at eastern SEISConn stations. Our interpretation of the NVG converter at mantle depths beneath SEISConn as perhaps corresponding to the LAB may provide additional support for the idea that the NAA may extend as far south as northern Connecticut, resulting in lithosphere that is as thin as ~60 km beneath the eastern end of SEISConn.

If this westward-dipping NVG converter beneath the central and eastern portion of the array (feature #5 in Figure 9) represents the LAB, then a natural question is whether the flat-lying NVG converter at ~75 km depth beneath the western (Laurentian) portion of the array (feature #6 in Figure 9) is also the LAB, or whether it has a different origin. Although a 75 km thick lithosphere seems very thin for Precambrian continental lithosphere (e.g., Steinberger & Becker, 2018), this value is approximately consistent with that estimated by Hopper and Fischer (2018) beneath this region based on Sp receiver functions. If this flat-lying converter is indeed the LAB, then there is a significant offset between this flat LAB in the west and west-dipping LAB to the east, which can be traced to a depth of ~90 km. The cause of this potential offset is obscure, although it might be a result the disturbance from the inferred relict slab (feature #4 in Figure 9), which in this interpretation penetrates the LAB and may have caused the LAB to locally deepen beneath it.

An alternative explanation for the flat NVG beneath the western part of the profile (feature #6 in Figure 9) is that it corresponds to a mid-lithospheric discontinuity (MLD) within (presumably thicker) Laurentian lithosphere. In this model, the lithosphere beneath Laurentia is likely considerably thicker than beneath the rest of the study area; it may be too deep to be reliably imaged using Ps receiver functions, or it may involve a velocity contrast that is too weak or diffuse to produce strong converted phases. Numerous studies have reported the existence of one or more sharp seismic velocity discontinuities at 50–100 km depth within the continental lithospheric mantle (e.g., Abt et al., 2010; Ford et al., 2016; Olugboji et al., 2016; Rader et al., 2015; Rychert & Shearer, 2009, 2011; Selway et al., 2015; Yuan & Romanowicz, 2010), known as MLDs; they appear to be a common, perhaps nearly universal, feature in continental lithosphere. The origin of MLDs is debated, with several possible models including anisotropic layering (e.g., Rychert & Shearer, 2009; Yuan & Romanowicz, 2010), chemical layering (e.g., Rader et al., 2015; Saha et al., 2021), and a transition to elastically accommodated grain-boundary sliding (EAGBS) (e.g., Karato & Park, 2019; Karato et al., 2015). Anisotropic layering models attribute observed seismic discontinuity to the systematic change of anisotropy with depth, caused by the change in flow geometry and the presence of partial melting (e.g., Yuan & Romanowicz, 2010). Chemical layering models invoke the presence of hydrous and/or carbonate mineral phases at mid-lithospheric depths in cratons to explain the velocity reduction at MLDs (e.g., Saha et al., 2021). Karato et al. (2015) proposed that the transition of deformation regime from purely elastic at lower temperatures to EAGBS at higher temperatures can result in the observed large seismic velocity drop without invoking any specific configurations of anisotropic and chemical layering. The EAGBS model is particularly interesting in the context of our imaging, as it may provide an explanation for the different features of the MLD/LAB beneath different portions of our study area. In this model, the transition to EAGBS in olivine is mostly controlled by temperature and will occur once a critical temperature (~1000°C) is reached. Beneath the (possibly) thick Precambrian lithosphere in the western part of Connecticut, the EAGBS model predicts an MLD between 50 and 100 km, where the critical temperature is reached and the transition to EAGBS causes a large velocity drop. Beneath the central and eastern portions of SEISConn, however, the lithosphere of Appalachian domains mantle is much thinner, perhaps as a result of the NAA asthenosphere upwelling. The shallow LAB may coincide with the transition to EAGBS, resulting in a large velocity drop at the LAB and strong Ps conversions, as observed. This model could be tested with future magnetotelluric studies of the lithosphere beneath southern New England, as it would predict a small change in electrical conductivity across the flat NVG in the west but a large increase in electrical conductivity across the west-dipping NVG to the east (Karato & Park, 2019).

5. Summary and Future Work

Our Ps receiver function imaging beneath Connecticut has revealed a variety of features that help to inform models for the tectonic evolution of the southern New England Appalachians. In particular, the dense (~10 km) station spacing of the SEISConn array has allowed for the imaging of structures on the short length scales that are relevant for comparisons with bedrock geologic structures. Major crustal structures that we image include the Moho itself, as well as the base of the Hartford sedimentary basin and a prominent west-dipping mid-crustal PVG converter. Crustal thickness across Connecticut varies from ~42 km in the west to ~27 km beneath the Hartford Basin, with the Moho gradually deepening to the east to ~35 km depth. We image a prominent "step" in the Moho that corresponds to the edge of Grenville (Laurentian) units at the surface; while this feature has been identified in previous studies (Li et al., 2018), the dense data coverage beneath SEISConn allows us to place tighter constraints on its geometry than have previously been possible. The Moho step may reflect general differences in crustal thickness between the Grenville Province and Appalachian domains (e.g., Levin et al., 2017), underthrusting of the Laurentian crust during the Taconic orogeny, or modification of crustal structure during later events, perhaps including the collapse of the Acadian Altiplano (Hillenbrand et al., 2021) or Mesozoic rifting. The west-dipping PVG converter in the crust probably represents one or more shear zones that reflect suturing during terrane accretion, with a likely association with the Salinic and/or Acadian orogenies. Features imaged at lithospheric mantle depths include a west-dipping PVG converter and one or more NVG features. The west-dipping PVG converter likely corresponds to the Moho of a relict slab; while the timing of this subduction event cannot be determined from seismic imaging alone, possibilities include subduction during (or just prior to) the Acadian, Neoacadian, or Alleghanian orogenies. The NVG converter may correspond to the base of the lithosphere beneath the central and eastern portions of the profile, suggesting a relatively shallow LAB that may have been affected by the low-velocity NAA in the upper mantle to the north. Beneath the western portion of the study area, the flat-lying NVG feature may correspond to an MLD within thicker Precambrian lithosphere, and the EAGBS model (Karato & Park, 2019) may successfully explain aspects of both the MLD and LAB beneath southern New England.

While the features identified in our receiver function imaging beneath SEISConn are robust, their interpretations remain uncertain, in large part because geophysics provides an image of present-day structure but no temporal information. We have suggested a number of plausible hypotheses to explain various features in this paper, but a major future challenge is to fully integrate seismic imaging with complementary structural, petrological, geochemical, geochronological, and paleomagnetic analyses, as well as with other types of geophysical imaging. Further seismological analyses to be conducted on SEISConn include detailed anisotropy-aware receiver function analysis that includes transverse component waveforms to more accurately constrain hypothesized crustal shear zones associated with terrane accretion, as well as a scattered wavefield migration analysis to better resolve multiple dipping structures observed in receiver function images. The integration of high-resolution geophysical images of the crust and mantle lithosphere beneath the southern New England Appalachians into models of tectonic evolution represents an exciting target for future work.

Acknowledgments
Collection and analysis of SEISConn data were funded by Yale University and by the National Science Foundation via grants EAR-1150722 and EAR-1800923. The authors thank the station hosts and field personnel who made the SEISConn experiment possible, particularly participants in the Field Experiences for Science Teachers (FEST) program (Long, 2017). Global Lithospheric Imaging with Earthquake Recordings (GLImER) was funded by a Marie Curie—Career Integration Grant 321871 from the European Commission FP7 Programme to Stéphane Rondenay. The authors are grateful to collaborators and colleagues on various aspects of SEISConn data analysis and other projects in New England for useful discussions, and the authors thank Shun-ichiro Karato for discussion on the MLD and the EAGBS model. The authors thank S. Gao and C. van Staal for thoughtful reviews that helped us to improve the study.

Data Availability Statement

Data used in this study are archived at the Incorporated Research Institutions for Seismology (IRIS) Data Management Center (DMC) and can be accessed at https://ds.iris.edu. All raw waveform data from the SEISConn experiment will be publicly available beginning in August 2021.

References

Abt, D. L., Fischer, K. M., French, S. W., Ford, H. A., Yuan, H., & Romanowicz, B. (2010). North American lithosphere discontinuity structure imaged by Ps and Sp receiver functions. *Journal of Geophysical Research*, *115*, 2009JB00691. https://doi.org/10.1029/2009jb006914

Bell, R. E., Karner, G. D., & Steckler, M. S. (1988). Early Mesozoic rift basins of eastern North America and their gravity anomalies: The role of detachments during extension. *Tectonics*, *7*(3), 447–462. https://doi.org/10.1029/tc007i003p00447

Benoit, M. H., Ebinger, C., & Crampton, M. (2014). Orogenic bending around a rigid Proterozoic magmatic rift beneath the central Appalachian Mountains. *Earth and Planetary Science Letters*, *402*, 197–208. https://doi.org/10.1016/j.epsl.2014.03.064

Birch, F. (1961). The velocity of compressional waves in rocks to 10 kilobars: 2. *Journal of Geophysical Research*, *66*(7), 2199–2224. https://doi.org/10.1029/jz066i007p02199

Bishop, B. T., Beck, S. L., Zandt, G., Wagner, L., Long, M., Antonijevic, S. K., et al. (2017). Causes and consequences of flat-slab subduction in southern Peru. *Geosphere*, *13*(5), 1392–1407. https://doi.org/10.1130/ges01440.1

Bogdanova, S. V., Pisarevsky, S. A., & Li, Z. X. (2009). Assembly and breakup of Rodinia (Some results of IGCP project 440). *Stratigraphy and Geological Correlation*, *17*(3), 259–274. https://doi.org/10.1134/s0869593809030022

Bonvalot, S., Balmino, G., Briais, A., Kuhn, M., Peyrefitte, A., Vales, N., et al. (2012). *World gravity map*. Bureau Gravimetrique International (BGI), Map, CGMW-BGI-CNES728IRD.

Brownlee, S. J., Schulte-Pelkum, V., Raju, A., Mahan, K., Condit, C., & Orlandini, O. F. (2017). Characteristics of deep crustal seismic anisotropy from a compilation of rock elasticity tensors and their expression in receiver functions. *Tectonics*, *36*(9), 1835–1857. https://doi.org/10.1002/2017tc004625

Condie, K. C. (2016). Chapter 2—The crust. In K. C. Condie (Ed.), *Earth as an evolving planetary system* (3rd ed., pp. 9–41). Academic Press. https://doi.org/10.1016/b978-0-12-803689-1.00002-x

Dewey, J. F. (1988). Extensional collapse of orogens. *Tectonics*, *7*(6), 1123–1139. https://doi.org/10.1029/tc007i006p01123

Domeier, M., & Torsvik, T. H. (2014). Plate tectonics in the late Paleozoic. *Geoscience Frontiers*, *5*(3), 303–350. https://doi.org/10.1016/j.gsf.2014.01.002

Eagar, K. C., & Fouch, M. J. (2012). FuncLab: A MATLAB interactive toolbox for handling receiver function datasets. *Seismological Research Letters*, *83*(3), 596–603. https://doi.org/10.1785/gssrl.83.3.596

Eaton, D. W., & Frederiksen, A. (2007). Seismic evidence for convection-driven motion of the North American plate. *Nature*, *446*(7134), 428–431. https://doi.org/10.1038/nature05675

Ford, H. A., Long, M. D., & Wirth, E. A. (2016). Midlithospheric discontinuities and complex anisotropic layering in the mantle lithosphere beneath the Wyoming and Superior Provinces. *Journal of Geophysical Research: Solid Earth*, *121*(9), 6675–6697. https://doi.org/10.1002/2016jb012978

Frizon de Lamotte, D., Fourdan, B., Leleu, S., Leparmentier, F., & de Clarens, P. (2015). Style of rifting and the stages of Pangea breakup. *Tectonics*, *34*(5), 1009–1029. https://doi.org/10.1002/2014tc003760

Gao, H., Yang, X., Long, M. D., & Aragon, J. C. (2020). Seismic evidence for crustal modification beneath the Hartford rift basin in the northeastern United States. *Geophysical Research Letters*, *47*(17), e2020GL089316. https://doi.org/10.1029/2020gl089316

Goldhagen, G., Ford, H. A., & Long, M. D. (2019). *Characterizing lithospheric structure beneath Connecticut using Sp receiver functions*. AGU.

Hatcher, R. D. (2002). *Alleghanian (Appalachian) orogeny, a product of zipper tectonics: Rotational transpressive continent-continent collision and closing of ancient oceans along irregular margins*. (pp. 199–208). Geological Society of America. https://doi.org/10.1130/0-8137-2364-7.199

Hatcher, R. D. (2010). The Appalachian orogen: A brief summary. In R. P. Tollo (Ed.), *From Rodinia to Pangea: The lithotectonic record of the Appalachian region*. (Vol. 206, pp. 1–19). Geological Society of America Memoir.

Hermes, O., & Murray, D. P. (1988). *Middle Devonian to Permian Plutonism and volcanism in the N American Appalachians* (Vol. 38, pp. 559–571). Geological Society, London, Special Publications. https://doi.org/10.1144/gsl.sp.1988.038.01.38

Hibbard, J. P., van Staal, C. R., Rankin, D. W., Tollo, R. P., Bartholomew, M. J., & Karabinos, P. M. (2010). Comparative analysis of the geological evolution of the northern and southern Appalachian orogen: Late Ordovician-Permian. In R. P. Tollo (Ed.), *From Rodinia to Pangea: The lithotectonic record of the Appalachian region*. Geological Society of America. https://doi.org/10.1130/2010.1206(03)

Hibbard, J. P., van Staal, C. R., Rankin, D. W., & Williams, H. (2006). *Lithotectonic map of the Appalachian Orogen*. Canada-United States of America. https://doi.org/10.4095/221912

Hillenbrand, I. (2020). *Crustal evolution of the New England Appalachians: The rise and fall of a long-lived orogenic plateau*. University of Massachusetts.

Hillenbrand, I. W., Williams, M. L., Li, C., & Gao, H. (2021). Rise and fall of the Acadian altiplano: Evidence for a Paleozoic orogenic plateau in New England. *Earth and Planetary Science Letters*, *560*, 116797. https://doi.org/10.1016/j.epsl.2021.116797

Hopper, E., & Fischer, K. M. (2018). The changing face of the lithosphere-asthenosphere boundary: Imaging continental scale patterns in upper mantle structure across the contiguous U.S. with Sp converted waves. *Geochemistry, Geophysics, Geosystems*, *19*(8), 2593–2614. https://doi.org/10.1029/2018gc007476

Hopper, E., Fischer, K. M., Wagner, L. S., & Hawman, R. B. (2017). Reconstructing the end of the Appalachian orogeny. *Geology*, *45*(1), 15–18. https://doi.org/10.1130/g38453.1

Hubert, J. F., Feshbach-Meriney, P. E., & Smith, M. A. (1992). The Triassic-Jurassic Hartford rift basin, Connecticut and Massachusetts: Evolution, sandstone diagenesis, and hydrocarbon history. *AAPG Bulletin*, *76*(11), 1710–1734. https://doi.org/10.1306/bdff8ab0-1718-11d7-8645000102c1865d

Hutchinson, D. R., Klitgord, K. D., Lee, M. W., & Tréhu, A. M. (1988). U.S. Geological Survey deep seismic reflection profile across the Gulf of Maine. *Geological Society of America Bulletin*, *100*(2), 172–184. https://doi.org/10.1130/0016-7606(1988)100<0172:usgsds>2.3.co;2

IRIS Transportable Array. (2003). *USArray transportable array*. International Federation of Digital Seismograph Networks.

Karabinos, P. (1997). *Does the northern termination of the Alleghanian fold and thrust belt record a reversal in subduction polarity?*. Geological Society of America.

Karabinos, P., Macdonald, F. A., & Crowley, J. L. (2017). Bridging the gap between the foreland and hinterland I: Geochronology and plate tectonic geometry of Ordovician magmatism and terrane accretion on the Laurentian margin of New England. *American Journal of Science*, *317*(5), 515–554. https://doi.org/10.2475/05.2017.01

Karabinos, P., Morris, D., Hamilton, M., & Rayner, N. (2008). Age, origin, and tectonic significance of Mesoproterozoic and Silurian felsic sills in the Berkshire massif, Massachusetts. *American Journal of Science*, *308*(6), 787–812. https://doi.org/10.2475/06.2008.03

Karabinos, P., Samson, S. D., Hepburn, J. C., & Stoll, H. M. (1998). Taconian orogeny in the New England Appalachians: Collision between Laurentia and the Shelburne Falls arc. *Geology*, *26*(3), 215–218. https://doi.org/10.1130/0091-7613(1998)026<0215:toitne>2.3.co;2

Karabinos, P. A., & Aleinikoff, J. N. (1990). Evidence for a major middle Proterozoic, post-Grenvillian igneous event in western New England. *American Journal of Science*, *290*(8), 959–974. https://doi.org/10.2475/ajs.290.8.959

Karato, S., & Park, J. (2019).On the origin of the upper mantle seismic discontinuities. In H. Yuan, & B. Romanowicz (Eds.), *Lithospheric disconstinuities* (pp. 5–34). American Geophysical Union.

Karato, S.-I., Olugboji, T., & Park, J. (2015). Mechanisms and geologic significance of the mid-lithosphere discontinuity in the continents. *Nature Geoscience*, *8*(7), 509–514. https://doi.org/10.1038/ngeo2462

Kay, A., Hepburn, J. C., Kuiper, Y. D., & Baxter, E. F. (2017). Geochemical evidence for a Ganderian arc/back-arc remnant in the Nashoba Terrane, SE New England, USA. *American Journal of Science*, *317*(4), 413–448. https://doi.org/10.2475/04.2017.01

Keller, D. S., & Ague, J. J. (2018). High-pressure granulite facies metamorphism (~1.8 GPa) revealed in silica-undersaturated garnet-spinel-corundum gneiss, Central Maine Terrane, Connecticut, U.S.A. *American Mineralogist*, *103*(11), 1851–1868.
Kennett, B. L. N., & Engdahl, E. R. (1991). Traveltimes for global earthquake location and phase identification. *Geophysical Journal International*, *105*(2), 429–465. https://doi.org/10.1111/j.1365-246x.1991.tb06724.x
Kind, R., Yuan, X., Saul, J., Nelson, D., Sobolev, S. V., Mechie, J., et al. (2002). Seismic images of crust and upper mantle beneath Tibet: Evidence for Eurasian plate subduction. *Science*, *298*(5596), 1219–1221. https://doi.org/10.1126/science.1078115
Kuiper, Y., Murray, D. P., Ellison, S., & Crowley, J. L. (2021). U-PB detrital zircon analysis of sedimentary rocks of the southeastern New England Avalon terrane in the US Appalachians: Evidence for a separate crustal block. *2021 Northeastern section meeting*. The Geological Society of America. https://doi.org/10.1130/abs/2021ne-361678
Kuiper, Y. D. (2018). Does West African crust extend into southeastern New England? *Paper presented at Northeastern Section-53rd Annual Meeting-2018*. GSA.
Kuiper, Y. D., Thompson, M. D., Barr, S. M., White, C. E., Hepburn, J. C., & Crowley, J. L. (2017). Detrital zircon evidence for Paleoproterozoic West African crust along the eastern North American continental margin, Georges Bank, offshore Massachusetts, USA. *Geology*, *45*(9), 811–814. https://doi.org/10.1130/g39203.1
Langston, C. A. (1979). Structure under Mount Rainier, Washington, inferred from teleseismic body waves. *Journal of Geophysical Research*, *84*(B9), 4749–4762. https://doi.org/10.1029/jb084ib09p04749
Leo, G. W., Mortensen, J. K., Barreiro, B., & Phillips, J. D. (1993). Petrology and U-Pb geochronology of buried Avalonian plutonic rocks on southeastern Cape Cod. *Atlantic Geology*, *29*(2), 103–113. https://doi.org/10.4138/1993
Levin, V., Long, M. D., Skryzalin, P., Li, Y., & López, I. (2018). Seismic evidence for a recently formed mantle upwelling beneath New England. *Geology*, *46*(1), 87–90. https://doi.org/10.1130/g39641.1
Levin, V., Servali, A., VanTongeren, J., Menke, W., & Darbyshire, F. (2017). Crust-mantle boundary in eastern North America, from the (oldest) craton to the (youngest) rift. In G. Bianchini, J. L. Bodinier, R. Braga, & M. Wilson (Eds.), *The crust-mantle and lithosphere-asthenosphere boundaries: Insights from xenoliths, orogenic deep sections, and geophysical studies*. Geological Society of America
Levin, V., VanTongeren, J. A., & Servali, A. (2016). How sharp is the sharp Archean Moho? Example from eastern Superior Province. *Geophysical Research Letters*, *43*(5), 1928–1933. https://doi.org/10.1002/2016gl067729
Li, A., Forsyth, D. W., & Fischer, K. M. (2003). Shear velocity structure and azimuthal anisotropy beneath eastern North America from Rayleigh wave inversion. *Journal of Geophysical Research*, *108*(B8). https://doi.org/10.1029/2002jb002259
Li, C., Gao, H., & Williams, M. L. (2020). Seismic characteristics of the eastern North American crust with Ps converted waves: Terrane accretion and modification of continental crust. *Journal of Geophysical Research: Solid Earth*, *125*(5), e2019JB018727. https://doi.org/10.1130/abs/2020se-344646
Li, C., Gao, H., Williams, M. L., & Levin, V. (2018). Crustal thickness variation in the northern Appalachian Mountains: Implications for the geometry of 3-D tectonic boundaries within the crust. *Geophysical Research Letters*, *45*(12), 6061–6070. https://doi.org/10.1029/2018gl078777
Li, X., Sobolev, S. V., Kind, R., Yuan, X., & Estabrook, C. (2000). A detailed receiver function image of the upper mantle discontinuities in the Japan subduction zone. *Earth and Planetary Science Letters*, *183*(3), 527–541. https://doi.org/10.1016/s0012-821x(00)00294-6
Li, Z. X., Bogdanova, S., Collins, A. S., Davidson, A., De Waele, B., Ernst, R. E., et al. (2008). Assembly, configuration, and break-up history of Rodinia: A synthesis. *Precambrian Research*, *160*(1), 179–210. https://doi.org/10.1016/j.precamres.2007.04.021
Ligorría, J. P., & Ammon, C. J. (1999). Iterative deconvolution and receiver-function estimation. *Bulletin of the Seismological Society of America*, *89*(5), 1395–1400.
Long, M. D. (2017). The field experiences for science teachers (FEST) program: Involving Connecticut high school science teachers in field seismology. *Seismological Research Letters*, *88*(2A), 421–429. https://doi.org/10.1785/0220160162
Long, M. D., & Aragon, J. C. (2020). Probing the structure of the crust and mantle lithosphere beneath the southern New England Appalachians via the SEISConn deployment. *Seismological Research Letters*, *91*(5), 2976–2986. https://doi.org/10.1785/0220200163
Long, M. D., Benoit, M. H., Aragon, J. C., & King, S. D. (2019). Seismic imaging of mid-crustal structure beneath central and eastern North America: Possibly the elusive Grenville deformation? *Geology*, *47*(4), 371–374. https://doi.org/10.1130/g46077.1
Lopes, E., Long, M. D., Karabinos, P., & Aragon, J. C. (2020). SKS splitting and upper mantle anisotropy beneath the southern New England Appalachians: Constraints from the dense SEISConn array. *Geochemistry, Geophysics, Geosystems*, *21*(12), e2020GC009401. https://doi.org/10.1029/2020gc009401
Luo, Y., & Korenaga, J. (2020). Efficiency of eclogite removal from continental lithosphere and its implications for cratonic diamonds. *Geology*, *49*(4), 438–441. https://doi.org/10.1130/g48204.1
Macdonald, F. A., Ryan-Davis, J., Coish, R. A., Crowley, J. L., & Karabinos, P. (2014). A newly identified Gondwanan terrane in the northern Appalachian Mountains: Implications for the Taconic orogeny and closure of the Iapetus Ocean. *Geology*, *42*(6), 539–542. https://doi.org/10.1130/g35659.1
Massey, M. A., Moecher, D. P., Walker, T. B., O'Brien, T. M., & Rohrer, L. P. (2017). The role and extent of dextral transpression and lateral escape on the post-Acadian tectonic evolution of south-central New England. *American Journal of Science*, *317*(1), 34–94. https://doi.org/10.2475/01.2017.02
Meert, J. G., & Van Der Voo, R. (1997). The assembly of Gondwana 800–550 Ma. *Journal of Geodynamics*, *23*(3), 223–235. https://doi.org/10.1016/s0264-3707(96)00046-4
Menke, W., Skryzalin, P., Levin, V., Harper, T., Darbyshire, F., & Dong, T. (2016). The Northern Appalachian anomaly: A modern asthenospheric upwelling. *Geophysical Research Letters*, *43*(19), 10173–10179. https://doi.org/10.1002/2016gl070918
Michard, A., Soulaimani, A., Hoepffner, C., Ouanaimi, H., Baidder, L., Rjimati, E. C., & Saddiqi, O. (2010). The south-western branch of the Variscan belt: Evidence from Morocco. *Tectonophysics*, *492*(1), 1–24. https://doi.org/10.1016/j.tecto.2010.05.021
Musacchio, G., Mooney, W. D., Luetgert, J. H., & Christensen, N. I. (1997). Composition of the crust in the Grenville and Appalachian Provinces of North America inferred from V_P/V_S ratios. *Journal of Geophysical Research: Solid Earth*, *102*(B7), 15225–15241. https://doi.org/10.1029/96jb03737
Nance, R. D., Gutiérrez-Alonso, G., Keppie, J. D., Linnemann, U., Murphy, J. B., Quesada, C., et al. (2012). A brief history of the Rheic Ocean. *Geoscience Frontiers*, *3*(2), 125–135. https://doi.org/10.1016/j.gsf.2011.11.008
Nance, R. D., & Linnemann, U. (2008). The Rheic Ocean: Origin, evolution, and significance. *Geological Society of America Today*, *18*(12), 4–12. https://doi.org/10.1130/gsatg24a.1
Nance, R. D., Murphy, J. B., Strachan, R. A., Keppie, J. D., Gutiérrez-Alonso, G., Fernández-Suárez, J., et al. (2008). *Neoproterozoic-early Palaeozoic tectonostratigraphy and palaeogeography of the peri-Gondwanan terranes: Amazonian v. West African connections* (Vol. 297, pp. 345–383). Geological Society, London, Special Publications. https://doi.org/10.1144/sp297.17

Olugboji, T. M., Park, J., Karato, S., & Shinohara, M. (2016). Nature of the seismic lithosphere-asthenosphere boundary within normal oceanic mantle from high-resolution receiver functions. *Geochemistry, Geophysics, Geosystems*, *17*, 1265–1282. https://doi.org/10.1002/2015gc006214

Parker, E. H., Jr, Hawman, R. B., Fischer, K. M., & Wagner, L. S. (2013). Crustal evolution across the southern Appalachians: Initial results from the SESAME broadband array. *Geophysical Research Letters*, *40*(15), 3853–3857. https://doi.org/10.1002/grl.50761

Pe-Piper, G., Kamo, S. L., & McCall, C. (2010). The German bank pluton, offshore SW Nova Scotia: Age, petrology, and regional significance for Alleghanian plutonism. *Bulletin of the Geological Society of America*, *122*(5–6), 690–700. https://doi.org/10.1130/b30031.1

Petrescu, L., Bastow, I. D., Darbyshire, F. A., Gilligan, A., Bodin, T., Menke, W., & Levin, V. (2016). Three billion years of crustal evolution in eastern Canada: Constraints from receiver functions. *Journal of Geophysical Research: Solid Earth*, *121*(2), 788–811. https://doi.org/10.1002/2015jb012348

Piana Agostinetti, N., Martini, F., & Mongan, J. (2018). Sedimentary basin investigation using receiver function: An East African rift case study. *Geophysical Journal International*, *215*(3), 2105–2113.

Porritt, R. W., & Miller, M. S. (2018). Updates to FuncLab, a Matlab based GUI for handling receiver functions. *Computers & Geosciences*, *111*, 260–271. https://doi.org/10.1016/j.cageo.2017.11.022

Rader, E., Emry, E. L., Schmerr, N., Frost, D., Cheng, C., Menard, J., et al. (2015). Characterization and petrological constraints of the midlithospheric discontinuity. *Geochemistry, Geophysics, Geosystems*, *16*, 3484–3504. https://doi.org/10.1002/2015gc005943

Rast, N., Skehan, J. W., Roy, D. C., & Skehan, J. W. (1993). Mid-Paleozoic orogenesis in the North Atlantic: The Acadian orogeny. In D. C. Roy, & J. W. Skehan (Eds.), *The Acadian orogeny: Recent studies in New England, maritime Canada, and the autochthonous foreland*. Geological Society of America. https://doi.org/10.1130/spe275-p1

Rivers, T. (1997). Lithotectonic elements of the Grenville Province: Review and tectonic implications. *Precambrian Research*, *86*(3), 117–154. https://doi.org/10.1016/s0301-9268(97)00038-7

Rivers, T. (2012). Upper-crustal orogenic lid and mid-crustal core complexes: Signature of a collapsed orogenic plateau in the hinterland of the Grenville Province. *Canadian Journal of Earth Sciences*, *49*(1), 1–42. https://doi.org/10.1139/e11-014

Robinson, P., Tracy, R., Hollocher, K., Berry, IV, H., & Thomson, J. (1989). Basement and cover in the Acadian metamorphic high of central Massachusetts. In J. B. Thompson, C. P. Chamberlain, & P. Robinson (Eds.), *Styles of Acadian metamorphism with depth in the central Acadian high* (pp. 69–140). Department of Geology and Geography, University of Massachusetts.

Robinson, P., Tucker, R. D., Bradley, D., Berry, H. N., & Osberg, P. H. (1998). Paleozoic orogens in New England, USA. *GFF*, *120*(2), 119–148. https://doi.org/10.1080/11035899801202119

Rondenay, S. (2009). Upper mantle imaging with array recordings of converted and scattered teleseismic waves. *Surveys in Geophysics*, *30*(4–5), 377–405. https://doi.org/10.1007/s10712-009-9071-5

Rondenay, S., Spieker, K., Sawade, L., Halpaap, F., & Farestveit, M. (2017). GLImER: A new global database of teleseismic receiver functions for imaging earth structure. *Seismological Research Letters*, *88*(1), 39–48. https://doi.org/10.1785/0220160111

Rychert, C. A., Fischer, K. M., & Rondenay, S. (2005). A sharp lithosphere-asthenosphere boundary imaged beneath eastern North America. *Nature*, *436*(7050), 542–545. https://doi.org/10.1038/nature03904

Rychert, C. A., Harmon, N., & Armitage, J. J. (2018). Seismic imaging of thickened lithosphere resulting from plume pulsing Beneath Iceland. *Geochemistry, Geophysics, Geosystems*, *19*(6), 1789–1799. https://doi.org/10.1029/2018gc007501

Rychert, C. A., Rondenay, S., & Fischer, K. M. (2007). P-to-S and S-to-P imaging of a sharp lithosphere-asthenosphere boundary beneath eastern North America. *Journal of Geophysical Research*, *112*(B8). https://doi.org/10.1029/2006jb004619

Rychert, C. A., & Shearer, P. M. (2009). A global view of the lithosphere-asthenosphere boundary. *Science*, *324*, 495–498. https://doi.org/10.1126/science.1169754

Rychert, C. A., & Shearer, P. M. (2011). Imaging the lithosphere-asthenosphere boundary beneath the Pacific using SS waveform modeling. *Journal of Geophysical Research*, *116*. https://doi.org/10.1029/2010JB0087010.1029/2010jb008070

Sacks, P. E., & Secor, D. T. (1990). Kinematics of late Paleozoic continental collision between Laurentia and Gondwana. *Science*, *250*(4988), 1702–1705. https://doi.org/10.1126/science.250.4988.1702

Saha, S., Peng, Y., Dasgupta, R., Mookherjee, M., & Fischer, K. M. (2021). Assessing the presence of volatile-bearing mineral phases in the cratonic mantle as a possible cause of mid-lithospheric discontinuities. *Earth and Planetary Science Letters*, *553*, 116602. https://doi.org/10.1016/j.epsl.2020.116602

Sawade, L. W. S. (2018). *Global common conversion point stacking and its applications*. The University of Bergen.

Selway, K., Ford, H. A., & Kelemen, P. (2015). The seismic mid-lithosphere discontinuity. *Earth and Planetary Science Letters*, *414*, 45–57. https://doi.org/10.1016/j.epsl.2014.12.029

Severson, A. R. (2020). *Across-and along-strike structural and geochronological variations of the Nashoba-Putnam and Avalon terranes, eastern Massachusetts, Connecticut, and Rhode Island, southeastern New England Appalachians*. Colorado School of Mines.

Simmons, N. A., Forte, A. M., Boschi, L., & Grand, S. P. (2010). GyPSuM: A joint tomographic model of mantle density and seismic wave speeds. *Journal of Geophysical Research*, *115*(B12). https://doi.org/10.1029/2010jb007631

Skehan, J. W., & Rast, N. (1990). Pre-Mesozoic evolution of Avalon terranes of southern New England. In A. D. Socci, J. W. Skehan, & G. W. Smith (Eds.), *Geology of the composite Avalon terrane of southern New England*. (Vol. 245, pp. 13–54). Geological Society of America Special Paper. https://doi.org/10.1130/spe245-p13

Steinberger, B., & Becker, T. W. (2018). A comparison of lithospheric thickness models. *Tectonophysics*, *746*, 325–338. https://doi.org/10.1016/j.tecto.2016.08.001

Stewart, D. B., Wright, B. E., Unger, J. D., Phillips, J. D., & Hutchinson, D. R. (1991). *Global geoscience transect 8, Quebec-Maine-Gulf of Maine transect, southeastern Canada, northeastern United States of America (Report)*. (Vol. 91–353). U.S. Geological Survey. https://doi.org/10.3133/ofr91353

Tao, Z., Li, A., & Fischer, K. M. (2020). Hotspot signatures at the North American passive margin. *Geology*, *49*(5), 525–530.

Thomas, W. A. (2006). Tectonic inheritance at a continental margin. *Geological Society of America Today*, *16*(2), 4–11. https://doi.org/10.1130/1052-5173(2006)016[4:tiaacm]2.0.co;2

Tollo, R. P., McLelland, J., Corriveau, L., & Bartholomew, M. J. (2004). *Proterozoic tectonic evolution of the Grenville orogen in North America*. Geological Society of America.

van der Velden, A. J., van Staal, C. R., & Cook, F. A. (2004). Crustal structure, fossil subduction, and the tectonic evolution of the Newfoundland Appalachians: Evidence from a reprocessed seismic reflection survey. *GSA Bulletin*, *116*(11–12), 1485–1498. https://doi.org/10.1130/b25518.1

van Staal, C. R., Whalen, J. B., Valverde-Vaquero, P., Zagorevski, A., & Rogers, N. (2009). Pre-Carboniferous, episodic accretion-related, orogenesis along the Laurentian margin of the northern Appalachians. *Geological Society, London, Special Publications*, *327*(1), 271–316. https://doi.org/10.1144/sp327.13

van Staal, C. R., Wilson, R. A., Kamo, S. L., McClelland, W. C., & McNicoll, V. (2016). Evolution of the early to middle Ordovician Popelogan arc in New Brunswick, Canada, and adjacent Maine, USA: Record of arc-trench migration and multiple phases of rifting. *GSA Bulletin*, *128*(1–2), 122–146.

Vinnik, L. P., Farra, V., & Kind, R. (2004). Deep structure of the Afro-Arabian hotspot by S receiver functions. *Geophysical Research Letters*, *31*(11). https://doi.org/10.1029/2004gl019574

Wagner, L. S., Stewart, K., & Metcalf, K. (2012). Crustal-scale shortening structures beneath the Blue Ridge Mountains, North Carolina, USA. *Lithosphere*, *4*(3), 242–256. https://doi.org/10.1130/l184.1

Wang, X., Zhao, D., Suzuki, H., Li, J., & Ruan, A. (2017). Eclogitization of the subducted oceanic crust and its implications for the mechanism of slow earthquakes. *Geophysical Research Letters*, *44*(24), 12225–12132. https://doi.org/10.1002/2017gl074945

Wenk, W. (1984). Seismic refraction model of depth of basement in the Hartford rift basin, Connecticut and Massachusetts. *Northeastern Geology*, *6*, 196–202. https://doi.org/10.1016/0191-8141(84)90007-5

White, C. E., Barr, S. M., Tollo, R. P., Bartholomew, M. J., Hibbard, J. P., & Karabinos, P. M. (2010). Lithochemistry of the lower Paleozoic Goldenville and Halifax groups, southwestern Nova Scotia, Canada: Implications for stratigraphy, provenance, and tectonic setting of the Meguma terrane. In R. P. Tollo (Ed.), *From Rodinia to Pangea: The lithotectonic record of the Appalachian region*. Geological Society of America. https://doi.org/10.1130/2010.1206(15)

Withjack, M., Malinconico, M., & Durcanin, M. (2020). The "passive" margin of eastern North America: Rifting and the influence of prerift orogenic activity on postrift development. *Lithosphere*, *2020*(1), 8876280.

Withjack, M. O., & Schlische, R. W. (2005). A review of tectonic events on the passive margin of eastern North America. Paper presented at *Petroleum Systems of Divergent Continental Margin Basins: 25th Bob S. Perkins Research Conference*. Gulf Coast Section of SEPM.

Withjack, M. O., Schlische, R. W., Olsen, P. E., Renaut, R. W., & Ashley, G. M. (2002). Rift-basin structure and its influence on sedimentary systems. In R. W. Renaut, G. M. Ashley (Eds.), *Sedimentation in continental rifts*. SEPM Society for Sedimentary Geology. https://doi.org/10.2110/pec.02.73.0057

Worthington, J. R., Hacker, B. R., & Zandt, G. (2013). Distinguishing eclogite from peridotite: EBSD-based calculations of seismic velocities. *Geophysical Journal International*, *193*(1), 489–505. https://doi.org/10.1093/gji/ggt004

Yuan, H., & Romanowicz, B. (2010). Lithospheric layering in the North American craton. *Nature*, *466*, 1063–1068. https://doi.org/10.1038/nature09332

Yuan, X., Sobolev, S. V., Kind, R., Oncken, O., Bock, G., Asch, G., et al. (2000). Subduction and collision processes in the Central Andes constrained by converted seismic phases. *Nature*, *408*(6815), 958–961. https://doi.org/10.1038/35050073

Zheng, T., Zhao, L., & Chen, L. (2005). A detailed receiver function image of the sedimentary structure in the Bohai Bay basin. *Physics of the Earth and Planetary Interiors*, *152*(3), 129–143. https://doi.org/10.1016/j.pepi.2005.06.011